

C_{arenium}–C_{alkyl} Bond Making and Breaking: Key Process in the Platinum-Mediated C_{aryl}–C_{alkyl} Bond Formation. Analogies to Organic Electrophilic Aromatic Substitution

Martin Albrecht,[†] Anthony L. Spek,^{‡,§} and Gerard van Koten^{†,*}

Contribution from the Debye Institute, Department of Metal-Mediated Synthesis, Utrecht University, and Bijvoet Center for Biomolecular Research, Crystal and Structural Chemistry, Utrecht University, Padualaan 8, 3584 CH Utrecht, The Netherlands

Received October 16, 2000

Abstract: The reaction of cationic platinum *aqua* complexes **2** [Pt(C₆H₂{CH₂NMe₂}₂-E-4)(OH₂)](X') (X' = SO₃CF₃, BF₄) with alkyl halides RX gave various air-stable arenium complexes **3–5** containing a new C–C bond (R = Me, **3**; Et, **4**; Bn, **5**). Electron-releasing oxo-substituents on the aromatic ligand (E = e.g., OH, **b**; OMe, **c**) enhance the reactivity of the *aqua* complex **2** and were essential for arenium formation from alkyl halides different from MeX. This process is initiated by oxidative addition of alkyl halides to the platinum(II) center of **2**, which affords (alkyl)(aryl) platinum(IV) complexes (e.g., **9**, alkyl = benzyl) as intermediates. Spectroscopic analyses provided direct evidence for a subsequent reversible 1,2-sigmatropic shift of the alkyl group along the Pt–C_{aryl} bond, which is identical to repetitive C_{arenium}–C_{alkyl} bond making and breaking and concerted metal reduction and oxidation. Temperature-dependent NMR spectroscopy revealed $\Delta H^\circ = -1.3$ (± 0.1) kJ mol⁻¹, $\Delta S^\circ = +3.8$ (± 0.2) J mol⁻¹ K⁻¹, and $\Delta G^\circ_{298} = -2.4$ (± 0.1) kJ mol⁻¹ for the formation of the arenium complex **5b** from **9** involving the migration of a benzyl group. The arenium complexes were transformed to cyclohexadiene-type addition products **7** or to demetalated alkyl-substituted arenes, **8**, thus completing the platinum-mediated formation of a sp²–sp³ C–C bond which is analogous to the aromatic substitution of a [PtX]⁺ unit by an alkyl cation R⁺. The formation of related trimethylsilyl arenium complexes **6** suggests arenium complexes as key intermediates, not only in (metal-mediated) sp²–sp³ C–C bond making and breaking but also in silyl-directed cyclometalation.

Introduction

The selective cleavage and formation of carbon–carbon bonds, in particular of sp²–sp³ C–C bonds, is of fundamental importance both to bulk chemical syntheses (oil chemistry, cracking processes) and to fine chemistry (natural product synthesis, pharmaceuticals).¹ The availability of powerful catalytic systems for these processes is crucial, in particular because of the high bond dissociation energy of such bonds (ca. 400 kJ mol⁻¹).² Appropriate catalysts are expected to provide access to selective and efficient bond cleavage and formation procedures which tolerate a large diversity of functional groups. Hence, considerable efforts have been devoted to the metal-mediated catalytic activation of C–C bonds in solution.³ Obviously, an appropriate understanding of the mechanism of these reactions is essential for the design of better catalysts.

A rational approach toward the mechanistic elucidation of the C_{aryl}–C_{alkyl} bond cleavage processes relies on the examination of the microscopic reverse, viz. C–C bond formation.

* To whom correspondence should be addressed. Fax: +31-30-2523615. E-mail: g.vankoten@chem.uu.nl.

† To whom correspondence pertaining to crystallographic studies should be addressed. E-mail: a.l.spek@chem.uu.nl.

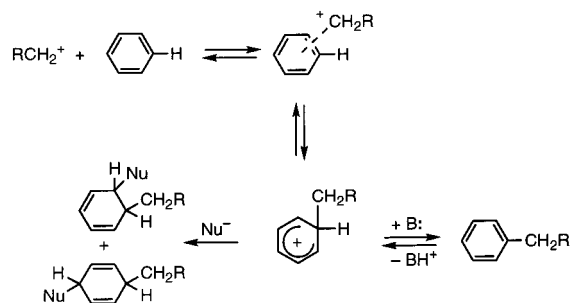
‡ Debye Institute.

§ Bijvoet Center.

(1) (a) Crabtree, R. H. *Chem. Rev.* **1985**, *85*, 245. (b) *Activation of Unreactive Bonds and Organic Synthesis*; Murai, S., Ed.; Springer: Berlin, 1999. (c) Jones, W. D. *Science* **2000**, *287*, 1942.

(2) Benson, S. *Thermochemical Kinetics*; Wiley: New York, 1976; p 309.

Scheme 1

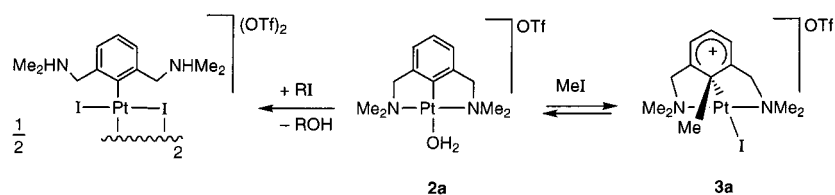


Formally, this reaction is analogous to Friedel–Crafts alkylation of arenes, a special case of electrophilic aromatic substitution (Scheme 1).⁴ The generally accepted mechanism includes trapping of the electrophile by an aromatic system under formation of a reactive encounter complex (π -complex). This species subsequently rearranges to a σ -complex (arenium, Wheland intermediate),⁵ which contains an activated C–H bond. In the final step, this activated proton is abstracted by a (weak)

(3) (a) Noyori, R.; Kumagai, Y.; Umeda, I.; Takaya, H. *J. Am. Chem. Soc.* **1972**, *94*, 4018. (b) Huffman, M. A.; Liebeskind, L. S. *J. Am. Chem. Soc.* **1991**, *113*, 2771. (c) Perthuisot, C.; Jones, W. D. *J. Am. Chem. Soc.* **1994**, *116*, 3647. (d) Edelbach, B. L.; Lachicotte, R. J.; Jones, W. D. *J. Am. Chem. Soc.* **1998**, *120*, 2843. (e) Rybtchinski, B.; Milstein, D. *Angew. Chem.* **1999**, *111*, 918; *Angew. Chem. Int. Ed.* **1999**, *38*, 870 and references therein. (f) Jia, C.; Piao, D.; Oyamada, J.; Lu, W.; Kitamura, T.; Fujiwara, Y. *Science* **2000**, *287*, 1992.

(4) Roberts, R. M.; Khalaf, A. A. *Friedel–Crafts Alkylation Chemistry*; Marcel Dekker: New York, 1984.

Scheme 2



base, thus affording a C-substituted benzene derivative containing a new carbon–carbon bond. Alternatively, a nucleophile can add to the arenium ion, thus giving 1,2- or 1,4-disubstituted cyclohexadiene addition products (Scheme 1).⁶

These reactivities underline the importance of the arenium intermediate as precursors for substituted arenes:⁷ its control allows the selective determination of the product formation and may be directed toward both, C–C bond cleavage (i.e., release of the alkyl unit) or toward C–C bond formation (i.e., release of a proton) or toward the addition product. Therefore, the characterization and isolation of arenium ions attracted particular interest and resulted in the spectroscopic identification of the very reactive benzenium ion C_6H_7^+ , the simplest member of the arenium family.⁸ Due to the sensitivity of this benzenium ion, its isolation has not been successful so far. In contrast, arenium ions with an enhanced stability, imposed by electron-releasing substituents such as in C_6Me_7^+ , have been isolated and fully characterized, including the X-ray structure determination.⁹

Among the first air-stable arenium ions was the metal-stabilized arenium **3a**, which has been prepared from MeI and the aromatic precursor **2a** (Scheme 2), a cationic platinum *solvento* complex containing the *N,C,N*-terdentate coordinating pincer ligand $[\text{C}_6\text{H}_3(\text{CH}_2\text{NMe}_2)_2-2,6]^-$ (abbreviated as NCN).^{10,11} Metal complexes of such “pincer” class ligands, that is, potentially terdentate chelating aryl-carbanions of the NCN-¹² or PCP-type,^{3e,13} are known for their outstanding properties in stabilizing unusual reaction intermediates and thus may provide insight into mechanistic details of such reactions.¹⁴

Due to its stability toward oxygen (i.e., air) and moderate heat, complex **3a** is an easily accessible model to study the

stability and reactivity of arenium (σ -complexes) key intermediates in electrophilic aromatic substitution chemistry.^{15,16} Cyanide-mediated removal of the metal in **3a** has been demonstrated to result in the formation of an alkyl-substituted arene¹⁰ (i.e., the product of $\text{C}_{\text{aryl}}-\text{C}_{\text{alkyl}}$ bond formation) thus identifying the arenium complex (i.e., $\text{C}_{\text{arenium}}-\text{C}_{\text{alkyl}}$ bond formation) as a potential intermediate of metal-mediated sp^2-sp^3 C–C bond making and breaking. Moreover, such arenium ions also represent frozen intermediates of electrophilic metalation reactions of arenes, which involve metal-mediated $\text{C}_{\text{aryl}}-\text{E}$ bond activation ($\text{E} = \text{H}, \text{C}, \text{Si}$).¹⁷ An elegant theoretical investigation suggested that proceeding to metal-stabilized arenium formation, an (aryl)(alkyl) metal complex with a formally oxidized metal center would be formed.^{10d} The more labile (alkyl) component subsequently migrates from the metal to the (aryl) *ipso*-carbon thus inducing arenium formation. Variation of the alkyl halide (RX) substrates for reaction with **2a** did, however, result in a cascade of reactions which slowly afford the corresponding alcohol (ROH) and an unusual zwitterionic platinum(II) dimer (Scheme 2).¹⁸ The proposed (alkyl)(aryl) metal complexes have been isolated in related rhodium chemistry where the corresponding arenium intermediates obviously are not sufficiently stable to be detected.¹⁹

Here, we present a successful approach to circumvent this restricted reactivity of arylplatinum complexes toward higher alkyl halide reactants, which identifies such arenium ion formation as an essential and general process in metal-mediated $\text{C}_{\text{aryl}}-\text{C}_{\text{alkyl}}$ bond activation. This approach relies on the introduction of electron-releasing substituents as activators on the aromatic ring (in this case on the NCN ligand), which is a classical concept derived from electrophilic aromatic substitution theory.⁴ These modifications allow for arenium formation (and hence $\text{C}_{\text{aryl}}-\text{C}_{\text{alkyl}}$ bond making) with various alkyl halides, which points to the existence of strong similarities between the metal-mediated sp^2-sp^3 C–C bond activation process and electrophilic aromatic substitution reactions. Moreover, direct evidence for the intimate steps of this reversible C–C bond-making and -breaking process has been obtained by using the cyclometalated NCN-“pincer” ligand. Preliminary results of

(5) (a) Olah, G. A. *Acc. Chem. Res.* **1971**, *4*, 250. (b) Ridd, J. H. *Acc. Chem. Res.* **1971**, *4*, 258. (c) Brouwer, D. M.; Mackor, E. L.; MacLean, C. In *Carbonium Ions*; Olah, G. A., Schleyer, P. v. R., Eds.; Wiley: New York, 1970; Vol. 2, p 837.

(6) (a) Corey, E. J.; Barcza, S.; Klotmann, G. *J. Am. Chem. Soc.* **1969**, *91*, 4782. (b) Hahn, R. C.; Strack, D. L. *J. Am. Chem. Soc.* **1974**, *96*, 4335.

(7) Canty, A. J.; van Koten, G. *Acc. Chem. Res.* **1995**, *28*, 406.

(8) (a) Olah, G. A.; Schlossberg, R. H.; Porter, R. D.; Mo, Y. K.; Kelly, D. P.; Mateescu, G. D. *J. Am. Chem. Soc.* **1972**, *94*, 2034. (b) Olah, G. A.; Staral, J. S.; Asencio, G.; Liang, G.; Forsyth, D. A.; Mateescu, G. D. *J. Am. Chem. Soc.* **1978**, *100*, 6299.

(9) (a) Oláh, G.; Kuhn, S.; Pavláth, A. *Nature* **1956**, *178*, 693. (b) Baenzinger, N. C.; Nelson, A. D. *J. Am. Chem. Soc.* **1968**, *90*, 6609. See also: (c) Rathore, R.; Hecht, J.; Kochi, J. K. *J. Am. Chem. Soc.* **1998**, *120*, 13278.

(10) (a) van Koten, G.; Timmer, K.; Noltes, J. G.; Spek, A. L. *J. Chem. Soc., Chem. Commun.* **1978**, 250. (b) Grove, D. M.; van Koten, G.; Louwen, J. N.; Noltes, J. G.; Spek, A. L.; Ubbels, H. J. C. *J. Am. Chem. Soc.* **1982**, *104*, 6609. (c) Terheijden, J.; van Koten, G.; Vinke, I. C.; Spek, A. L. *J. Am. Chem. Soc.* **1985**, *107*, 2891. For an early computational study of the process involved in the formation of these unique arenium species, see: (d) Ortiz, J. V.; Havlas, Z.; Hoffmann, R. *Helv. Chim. Acta* **1984**, *67*, 1.

(11) The term “arenium” is preferred to “arenonium”, as used by us earlier [see ref 10]. For a discussion of this nomenclature, see: Olah, G. A. *J. Am. Chem. Soc.* **1972**, *94*, 808.

(12) (a) van Koten, G. *Pure Appl. Chem.* **1989**, *61*, 1681. (b) Rietveld, M. P. H.; Grove, D. M.; van Koten, G. *New J. Chem.* **1997**, *21*, 751.

(13) (a) Moulton, C. J.; Shaw, B. L. *J. Chem. Soc., Dalton Trans.* **1976**, 1020. (b) Rimmel, H.; Venanzi, L. M. *J. Organomet. Chem.* **1983**, *259*, C6. (c) Nemeh, S.; Jensen, C.; Binamira-Soriaga, E.; Kaska, W. C. *Organometallics* **1983**, *2*, 1447. (d) Karlen, T.; Dani, P.; Grove, D. M.; Steenwinkel, P.; van Koten, G. *Organometallics* **1996**, *15*, 5687.

(14) (a) Gossage, R. A.; Ryabov, A. D.; Spek, A. L.; Stufkens, D. J.; van Beek, J. A. M.; van Eldik, R.; van Koten, G. *J. Am. Chem. Soc.* **1999**, *121*, 2488. (b) Dani, P.; Karlen, T.; Gossage, R. A.; Kooijman, H.; Spek, A. L.; van Koten, G. *J. Am. Chem. Soc.* **1997**, *119*, 11317. (c) van der Boom, M. E.; Higgitt, C. L.; Milstein, D. *Organometallics* **1999**, *18*, 2413. (d) Albrecht, M.; Dani, P.; Lutz, M.; Spek, A. L.; van Koten, G. *J. Am. Chem. Soc.* **2000**, *122*, 11822. (e) Vignalok, A.; Milstein, D. *J. Am. Chem. Soc.* **1997**, *119*, 7873. (f) Vignalok, A.; Shimon, L. J. W.; Milstein, D. *J. Am. Chem. Soc.* **1998**, *120*, 477.

(15) Grove, D. M.; van Koten, G.; Ubbels, H. J. C. *Organometallics* **1982**, *1*, 1366.

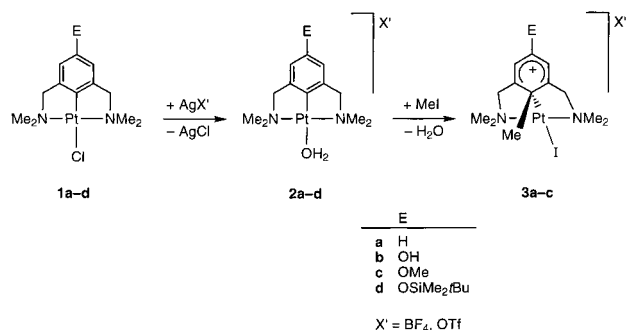
(16) (a) Pfeiffer, P.; Wizinger, R. *Liebigs Ann. Chem.* **1928**, *461*, 132. (b) Wheland, G. W. *J. Am. Chem. Soc.* **1942**, *64*, 900. (c) Farcasiu, D. *Acc. Chem. Res.* **1982**, *15*, 46.

(17) Cope, A. C.; Friedrich, E. C. *J. Am. Chem. Soc.* **1968**, *90*, 909.

(18) Davidson, M. F.; Grove, D. M.; Spek, A. L.; van Koten, G. *J. Chem. Soc., Chem. Commun.* **1989**, 1562.

(19) (a) Liou, S.-Y.; Gozin, M.; Milstein, D. *J. Am. Chem. Soc.* **1995**, *117*, 9774. (b) Rybtchinski, B.; Vignalok, A.; Ben-David, Y.; Milstein, D. *J. Am. Chem. Soc.* **1996**, *118*, 12406.

Scheme 3



these studies have been communicated recently.²⁰ Extended investigations now provide a general understanding for the mechanism of homogeneous metal-mediated C_{aryl}-C_{alkyl} bond making and breaking. Extension of our studies to transition metal-mediated C_{aryl}-Si (and C_{aryl}-H) bond activation showed that the developed mechanistic concept is of broad validity.

Results

Reaction of chloroplatinum complexes of the type [PtCl(NCN-E-4)] (E = H, OR), **1a-d**, with a silver salt (trifluoromethane sulfonate (OTf) or BF₄) in wet acetone results in quantitative abstraction of the chloride ligand and precipitation as silver chloride.^{10b,21} The open coordination site on the metal is filled by a water molecule thus yielding the cationic arylplatinum(II) *aqua* complexes [Pt(NCN-E-4)(OH₂)]⁺ with either OTf or BF₄ as anions (Scheme 3).²² These complexes **2a-d** were isolated as colorless solids in more than 85% yield. Coordinated water appears in their ¹H NMR spectra as a broad singlet at approximately 2.8 ppm. Interestingly, **2b** possesses hydrophilic groups at either end of the molecule, and consequently, this complex represents a water-soluble organoplatinum species. The hydroxyl group appears at 7.99 ppm and the coordinated water as a broad peak centered at 2.83 ppm (acetone solution). In the ¹H NMR spectra of all the *aqua*-complexes, the signals due to coordinated water or phenolic hydroxyl groups disappear on addition of D₂O. In addition, ¹H-¹⁹⁵Pt couplings of the NMe₂ and the CH₂N protons of the ligands are observed, the coupling constants of the latter being substantially larger than those found for the corresponding neutral complexes (50–52 Hz in **2** vs 40–46 Hz in **1**).

Methyl Arenium Complexes. The *aqua*-complexes **2a-d** undergo a characteristic color change to dark red when treated with MeI (λ_{max} ca. 460 nm in acetone). This color is indicative for the formation of a cationic arenium complex (Scheme 3).¹⁰ The methyl arenium species **3a-c** are obtained quantitatively and analytically pure by evaporation of all volatiles in vacuo and subsequent recrystallization of the product from a CH₂Cl₂ solution by slow diffusion of pentane. Despite of their ionic character, these complexes are highly soluble in acetone and CH₂Cl₂, to a lesser extent as well in EtOAc and CHCl₃. However, they do not dissolve in alkane solvents and benzene or toluene.

The ¹H NMR spectra of these cationic complexes are characteristic: in **3b**, for example, C–C bond formation is

(20) Albrecht, M.; Gossage, R. A.; Spek, A. L.; van Koten, G. *J. Am. Chem. Soc.* **1999**, *121*, 11898.

(21) (a) Terheijden, J.; van Koten, G.; Muller, F.; Grove, D. M.; Vrieze, K.; Nielsen, E.; Stam, C. H. *J. Organomet. Chem.* **1986**, *315*, 401. (b) Albrecht, M.; Gossage, R. A.; Lutz, M.; Spek, A. L.; van Koten, G. *Chem. Eur. J.* **2000**, *6*, 1431.

(22) Schmülling, M.; Grove, D. M.; van Koten, G.; van Eldik, R.; Veldman, N.; Spek, A. L. *Organometallics* **1996**, *15*, 1384.

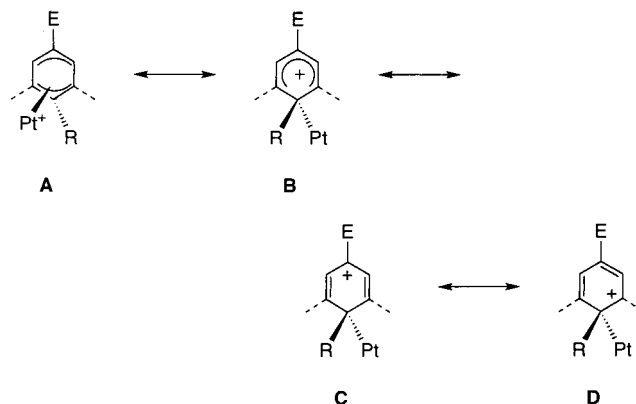


Figure 1. Resonance structures of the π -complex **A** and the arenium complexes **B–D** containing an activating substituent (E = OH, OMe).

indicated by a new CH₃ resonance at 2.70 ppm. In addition, two distinct singlets for the NCH₃ protons (at 3.14 and 2.82 ppm, respectively) and two AB doublets for the benzylic ArCH₂N protons (centered at 4.94 and 3.63 ppm) have been observed. This remarkably large chemical shift difference of 1.3 ppm together with the presence of vicinal ¹H-¹H couplings (²J = 13.4 Hz) implies a reduced symmetry of the molecular geometry and a fixed conformation of the ligand unit. Obviously, dynamic puckering processes as established for neutral arylplatinum complexes of the type [PtX(NCN-E-4)] are absent.^{10b,21} Further indications for a lower symmetry arises from examination of the coupling constants due to ¹H-¹⁹⁵Pt interactions. In **3b**, the coupling constants of the two chemically inequivalent benzylic protons vary considerably (29.4 vs 38.6 Hz), which is presumably induced by different dihedral angles of the Pt–N–C–H skeleton. Furthermore, the signals due to the aromatic protons shift from ca. 6.5 ppm (*aqua*-complexes **2b** and **2c**) downfield (to 7.07 and 7.28 ppm in **3b** and **3c**, respectively) upon C–C bond formation, suggesting a decreased electron density of the aryl fragment.

Principally, two different types of structures must be considered for these complexes: first, π -complexes, which contain a platinum center that is η^1 - or η^3 -coordinated to the arene unit (**A**, Figure 1; a classical η^6 -coordination mode is probably not accessible due to the strongly chelating amino groups), and second, σ -complexes (arenium), which comprise a Pt–C σ -bond (**B**, Figure 1). Due to the continuum of π - and σ -complexes,²³ either term often represents an approximative description of the effective structure only. On the basis of various structural information (vide infra) the herein reported complexes unambiguously show a η^1 -coordination mode and have been assigned to be arenium structures rather than π -complexes and are therefore referred to as arenium ions.²⁴

A more detailed insight into the electronic nature of the methyl arenium cations **3a-c** is gained by ¹³C {¹H} NMR spectroscopy. In **3a**, where para substituents are lacking, the *ipso*-carbon is shifted upfield to 102 ppm (from ca. 140 ppm in **1a** or **2a**), indicating a considerable change of the hybridization from sp² toward sp³. Furthermore, all of the other aryl-carbons show resonance signals between 135 and 145 ppm and support a structure containing an unperturbed aromatic system for this C₅ fragment of the ring, comprising a delocalized positive charge

(23) (a) Reed, C. A. *Acc. Chem. Res.* **1998**, *31*, 325. (b) Hubig, S. M.; Kochi, J. K. *J. Org. Chem.* **2000**, *65*, 6807.

(24) For a more detailed discussion concerning the σ - and π -bond contribution in the platinum-stabilized structures, see Supporting Information; for a general discussion, see ref 23 and Hubig, S. M.; Lindeman, S. V.; Kochi, J. K. *Coord. Chem. Rev.* **2000**, *200–202*, 831.

(Figure 1, structure **B**). This contrasts with the findings from measurements on **3b** and **3c**, which both contain an oxo-substituent on the aryl ring. In these complexes, the resonance of C_{ipso} is highfield-shifted (δ_{C} between 80 and 85 ppm) and appears in a region typical for (substituted) alkanes rather than for aryl carbons. This demonstrates a much higher degree of sp^3 hybridization of this carbon when compared to C_{ipso} in **3a** (cf. **B–D** in Figure 1). Moreover, the signals due to the *para*- and *ortho*-carbons in **3b** are remarkably deshielded ($\delta_{\text{C}} = 172.1$ and 155.7 , respectively), whereas the resonances of C_{meta} appears at lower frequency ($\delta_{\text{C}} = 117.4$). These chemical shift values strongly resemble those found in related (but very unstable) methoxy-substituted benzenium ions.²⁵ On the basis of these data, a structure in solution is surmised which is characterized by a partial localization of the positive charge at the *para* and *ortho* positions of the arenium system in **3b** (Figure 1, structures **C**, **D**). Similar results are obtained from spectroscopic analyses of the methyl arenium **3c**, and hence, both of these oxo-substituted arenium ions have significant α,β -unsaturated ketone-type character. Such a model corroborates the chemical shift values of the oxo-bound aryl-carbons, which appear at a frequency typical for ketones.

A different reactivity pattern was established for the cationic *aqua*-complex **2d** containing a siloxy substituent on the pincer ligand ($E = \text{OSiMe}_2/\text{Bu}$) in the presence of MeI. Formation of an arenium species is strongly indicated by the diagnostic dark red color of the reaction solution. The isolated product revealed a signal pattern in the ^1H NMR spectrum which is characteristic for arenium complexes (inequivalent NMe_2 and CH_2N protons, vide supra). Surprisingly, however, the resonances due to the SiMe_2/Bu group were entirely absent. Further analyses (UV-vis, ^{13}C $\{^1\text{H}\}$ NMR) confirmed cleavage of the Si–O bond and formation of **3b** (containing an unsubstituted phenol) rather than the corresponding *O*-silylated arenium cation. Activation of the Si–O bond is presumably supported by the constructive overlap of the leaving group properties of the silyl unit and of keto-enol tautomerization of both the arenium product and acetone, which has been used as solvent (Figure 1). This emphasizes indirectly the significance of a ketone-like arenium in the oxo-substituted systems rather than a charge-delocalized cation as found in **3a** (vide supra).

Solid-State Structure of [PtI(NCN-Me-1-OMe-4)][OTf] **3c.** The precise molecular geometry of the arenium **3c** has been unequivocally determined by single-crystal X-ray studies. Dark red plates of **3c** were grown by slow diffusion of pentane into a CHCl_3 solution containing **3c**. The molecular structure of **3c** (Figure 2) displays characteristics similar to those found for related arenium species. The platinum center is in a slightly distorted square-planar geometry with the nitrogen donors in mutual *trans* position (N1–Pt–N2 $170.7(3)^\circ$, Table 1). The fourth coordination site of the platinum center is occupied by iodide, originating from the activation of the $\text{CH}_3\text{–I}$ bond. A tetrahedral environment around the *ipso*-carbon is indicated by the pertinent angles of the four substituents varying between $103.9(5)^\circ$ and $120.2(8)^\circ$. This suggests sp^3 rather than sp^2 hybridization at this carbon. Further evidence for such a model was taken from the Pt–C1 bond length ($2.127(8)$ Å), which is substantially longer than in arylplatinum(II) complexes containing a fully sp^2 hybridized metal-bound carbon (typically in the range of 1.90 to 1.96 Å). The C_6 ring shows a boatlike conformation (torsion angle C2–C1–C6–C5 is $14.3(12)^\circ$) and forms an angle of 112.4° with the platinum coordination plane,

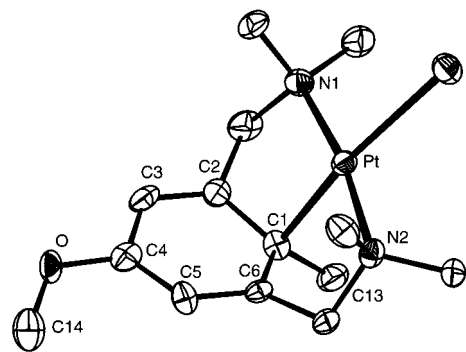


Figure 2. Perspective view (ORTEP, 50% probability) of the methyl arenium cation **3c**. Hydrogen atoms and the OTf^- anion were omitted for clarity.

Table 1. Selected Bond Length (Å) and Angles (deg) for Arenium Complexes **3c**, **5b**,^a and **5c**

	3c (X = I)	5b (X = Br)	5c (X = Br)
bond lengths			
Pt–X	2.6247(8)	2.4383(5)	2.4304(9)
Pt–N1	2.100(8)	2.090(4)	2.079(5)
Pt–N2	2.103(8)	2.100(4)	2.071(6)
Pt–C1	2.127(8)	2.106(4)	2.129(6)
C1–C13	1.541(12)	1.538(7)	1.535(8)
C1–C2	1.443(13)	1.445(6)	1.453(8)
C2–C3	1.365(13)	1.376(7)	1.375(8)
C3–C4	1.381(14)	1.402(7)	1.386(8)
C4–C5	1.399(14)	1.396(7)	1.415(8)
C5–C6	1.384(12)	1.370(7)	1.354(8)
C6–C1	1.440(13)	1.436(7)	1.453(8)
C4–O	1.339(11)	1.327(6)	1.350(7)
bond angles			
Pt–C1–C13	103.9(5)	112.2(3)	107.2(4)
C2–C1–C13	120.2(8)	117.4(4)	120.3(5)
C6–C1–C13	118.3(8)	119.4(4)	119.7(5)
C6–C1–C2	115.0(7)	114.8(4)	114.8(5)
C1–Pt–X	169.9(2)	177.97(14)	174.60(15)
N1–Pt–X	94.7(2)	92.91(12)	93.40(14)
N2–Pt–X	94.1(2)	93.68(12)	93.32(17)
N1–Pt–C1	86.0(3)	86.22(16)	87.4(2)
N2–Pt–C1	86.0(3)	87.19(16)	85.9(2)
N1–Pt–N2	170.7(3)	173.41(17)	173.3(2)
torsion angles			
C1–C2–C3–C4	–2.2(13)	1.6(7)	1.4(10)
C2–C1–C6–C5	14.3(12)	10.9(6)	13.2(9)
C2–C3–C4–O	–169.0(8)	–174.2(2)	–175.7(7)
Pt–C1–C6–C5	113.5(8)	106.9(4)	106.6(6)
C13–C1–C2–C3	138.7(9)	136.3(5)	141.6(6)
Pt–C1–C2–C3	–111.5(8)	–105.5(4)	–107.3(6)

^a From ref 20.

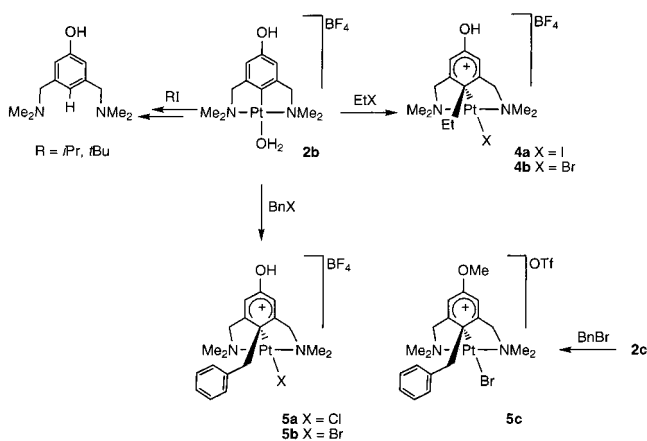
thus preventing the postulation of any type of agostic interaction²⁶ or (η^3 or exocyclic η^2) π -bonding.^{14f,23} Remarkably, the bond lengths between C2, C3, C4, and C5 are all in the range of 1.36–1.40 Å and deviate only slightly from the typical C–C bond length in unperturbed aromatic systems (1.38 Å). The bonds to the *ipso*-carbon are considerably stretched (1.44 Å), however, which is in good agreement with an arenium structure. The C–O bond length (C4–O 1.34 Å) relates well with those found for other similar structures and is too long for a ketone-type bond (typically around 1.24 Å).^{25,27}

Arenium Complexes from Activation of RX (R not Me). Earlier studies related to oxidative addition of alkyl halides to

(25) Olah, G. A.; Porter, R. D.; Jeuell, C. L.; White, A. M. *J. Am. Chem. Soc.* **1972**, *94*, 2044.

(26) (a) Brookhart, M.; Green, M. L. H.; Wong, L. L. *Prog. Inorg. Chem.* **1988**, *36*, 1. (b) Crabtree, R.; Hamilton, D. G. *Adv. Organomet. Chem.* **1988**, *28*, 299. (c) Dani, P.; Karlen, T.; Gossage, R. A.; Smeets, W. J. J.; Spek, A. L.; van Koten, G. *J. Am. Chem. Soc.* **1997**, *119*, 11317. (d) Vigalok, A.; Uzan, O.; Shimon, L. J. W.; Ben-David, Y.; Martin, J. M. L.; Milstein, D. *J. Am. Chem. Soc.* **1998**, *120*, 12539.

Scheme 4



arylplatinum(II) complexes containing NCN-type pincer ligands have shown that arenium formation takes place solely when the electrophile is a methyl cation. However, when larger alkyl halides RX such as ethyl (Et), isopropyl (iPr), or benzyl (Bn) were used, complex **2a** undergoes a cascade of reactions to form eventually the corresponding alcohol ROH along with an unprecedented zwitterionic dimetallic Pt(II) dication (Scheme 2).¹⁸ In contrast to **2a**, the oxo-substituted aqua-complexes **2b–d** possess a sufficiently activated arene system to react with various alkyl halides.

For example, addition of EtI to **2b** in acetone solution gave, after 24 h, the corresponding ethyl arenium complex **4a**, which was isolated after repeated dissolution in acetone and precipitation with Et₂O in good yields (Scheme 4). The spectral data are similar to those discussed for the methyl arenium analogue **3b**, except that the signal due to the C_{ipso}-bound methyl group in the ¹H NMR located at 2.70 ppm was absent, and instead, a quartet and a triplet (assigned to the ethyl group) appeared at 3.53 and 0.64 ppm, respectively. A similar reaction using excess of EtBr as alkylating agent gave **4b** but proceeded much more slowly and was not complete even after 15 days of reaction, while arenium formation of **4a** with the corresponding alkyl iodide was complete within 24 h. Consequently, formation of EtOH and the bromide analogue of the zwitterionic dimer shown in Scheme 2 became a strongly competitive process. This was most obvious in the ¹H NMR spectrum of the crude reaction mixture, which revealed the dimeric species (doublets at 4.55 ppm and at 3.09 ppm, for the benzylic and the methyl protons, respectively, of the CH₂NHMe₂ substituent¹⁸) as the predominant product. Increase in reaction temperature did neither significantly accelerate the reaction nor change the product distribution.

When the aqua complex **2b** was treated with benzyl halides (BnX; X = Cl, Br) the corresponding benzyl arenium complexes **5** were obtained (**5a**, X = Cl, **5b** X = Br). The reaction with BnBr proceeded much faster than with BnCl and was complete within 1 h. Hence, addition of BnBr to a colorless solution of **2** caused a rapid color change of the solution to dark purple (within several minutes) and then slowly to orange. After 1 h, UV–vis photospectroscopy indicated the reaction to be complete. The pertinent NMR and UV–vis data strongly resemble those of related alkyl arenium complexes (**3b**, **4b**) and are consistent with the formation of a benzyl arenium ion. Most characteristically, the benzylic protons of the Bn group appear

as a singlet at 4.46 ppm. Similar to the corresponding methyl arenium complex **3b**, the *meta*-carbons are considerably shielded ($\delta_C = 118.4$), but not the *ortho*- and *para*-carbons ($\delta_C = 157.5$, C_{ortho}; 172.5, C_{para}), and C_{ipso} has strong sp³ character ($\delta_C = 79.8$). The formation of the chloride analogue of this benzyl arenium complex, viz. **5a**, was much slower and did not proceed quantitatively. The spectroscopic characteristics are strongly related to those found for the analogous bromide complex **5b**. Similar reactivities were observed for the methoxy-substituted arylplatinum complex **2c**. In the presence of BnBr, a consecutive color change to purple and finally to orange indicated a reaction that is strongly related to the one starting from **2b**. Spectroscopic analysis of the product revealed essentially the same NMR resonances for **5c** and **5b**, containing a methoxy- and a hydroxy-substituent, respectively. The most characteristic difference in the ¹H NMR spectrum is the presence of a singlet at $\delta_H = 4.21$, assigned to the MeO-group in **5c**. Notably, this resonance is at significantly lower field than would be expected for methyl aryl ether signals (e.g., $\delta_H = 3.73$ ppm in **2c**), pointing to a strong electron-deficiency on the aryloxy unit. This is in agreement with the proposed charge distribution in such platinum-stabilized arenium systems.

Any of the cationic aqua-complexes **2** is inert toward the presence of excess of aryl iodides (I–C₆H₄–R'-4), irrespective on the nature of the substituent R'. Variation of the electronic influence of R' from strongly withdrawing (R' = CHO) to neutral (R' = H) or releasing (R' = OMe) did not induce any reaction. Also, addition of bulkier alkyl halides (e.g., ^tPrI or ^tBuI) to **2b** or **2c** did not cause formation of any stable arenium product. Instead of the characteristic red colored solution, a dark brown reaction mixture was obtained. Analyses (¹H NMR spectroscopy) showed the presence of the ligand moiety which lacked any platinum satellites thus indicating Pt–N bond fission. Moreover, two singlets were found in the aryl region at similar positions as those of the free ligand precursor. This is in accordance with platinum–carbon bond cleavage and protonation of C_{ipso}. Hence, a cascade of reactions involving oxidative addition and reductive elimination sequences is likely to have occurred, leading to the protonated metal-free ligand NCHN-E and most probably to a PtI₄-type fragment. These reaction products are in agreement with the observed dark brown color obtained during the process, which indicate the presence of molecular I₂, which is anticipated to origin from the added alkyl halide.

Using silyl chlorides (e.g., Me₃SiCl) as reagents with the aqua complexes **2a–d** resulted in the quantitative formation of the neutral arylplatinum complexes **1a–d** rather than arenium formation. This reaction pathway was successfully suppressed, however, when the neutral complex **1** and a more electrophilic silyl-cation were used as starting materials. Hence, treatment of the iodo-analogue of complex **1d**, that is [PtI(NCN–OSiMe₂^t-Bu)],^{21b} with excess Me₃SiOTf in anhydrous CH₂Cl₂ afforded an immediate color change of the reaction solution from colorless to dark red ($\lambda_{max} = 465$ nm), indicative for arenium systems comprising a metal-bound iodide.^{10c} Similarly, the ¹H NMR spectrum of this solution showed a signal pattern characteristic for arenium systems: two AB doublets appeared at 4.25 and 3.40 ppm and also, two inequivalent NMe groups were observed at 3.04 and 2.72 ppm, respectively. All these results are in good agreement with the formation of a new Si–C bond as postulated in the arenium complex **6a** (Scheme 5). Unambiguous evidence for the presence of a trimethylsilyl arenium ion was obtained from ²⁹Si NMR spectroscopy. The resonance signal at 78.9 ppm is in excellent agreement with the calculated values for related

(27) (a) Davies, P. J.; Veldman, N.; Grove, D. M.; Spek, A. L.; Lutz, B. T. G.; van Koten, G. *Angew. Chem.* **1996**, *108*, 2078; *Angew. Chem., Int. Ed. Engl.* **1996**, *35*, 1959. (b) Vagedes, D.; Fröhlich, R.; Erker, G. *Angew. Chem.* **1999**, *111*, 3561; *Angew. Chem., Int. Ed. Engl.* **1999**, *38*, 3362.

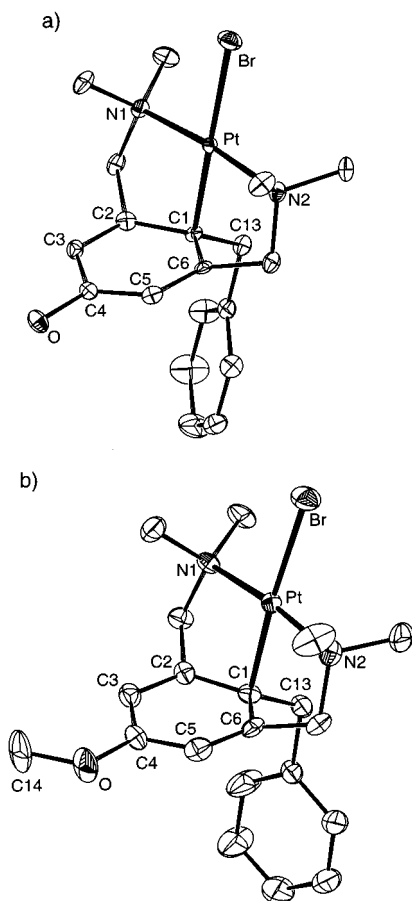
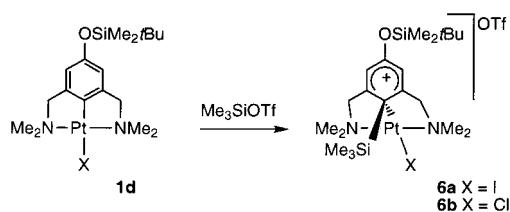


Figure 3. Perspective view (ORTEP, 50% probability) of the benzyl arenium cations **5b** (a) and **5c** (b). Hydrogen atoms, the anions (**5b**: BF_4^- ; **5c**: OTf^-), and disordered solvent molecules (**5c**) were omitted for clarity.

Scheme 5



silyl arenium ions and rules out the presence of a silyl cation (vide infra).²⁸ The proposed complex **6a** is highly reactive and unstable in the solid state. Any attempts to isolate **6a**, for example by precipitation or by crystallization under strictly anhydrous conditions, yielded the neutral arylplatinum complex **1d** (as its iodide analogue) together with some unidentified brown residue. When the chloride complex **1b** was used, an immediate evolution of a dark yellow color was noted ($\lambda_{\text{max}} = 435 \text{ nm}$), typical for platinum-stabilized arenium systems containing a metal-bound chloride ligand.^{10c} Spectroscopic measurements supported the formation of the trimethylsilyl arenium complex **6b**. However, also solid **6b** decomposed rapidly and could therefore neither be isolated nor purified.

Solid-State Structures of Benzyl Arenium Complexes 5b and 5c. The molecular structures of **5b** (Figure 3a)²⁰ and **5c** (Figure 3b) are similar in many respects. In both complexes,

the square-planar platinum(II) center is ligated by the terdentate chelating pincer ligand and by bromide, which is located in mutual *trans* position to the metal-bound carbon. The arenium ring is considerably tilted with respect to the metal coordination plane (105° in both structures, Table 1). The geometry at the *ipso*-carbon has significant tetrahedral character with all the bond angles with vertex C1 close to 109° , suggesting considerable sp^3 -type hybridization at C_{ipso} . The bonds to C6 and C2 are significantly stretched (1.44–1.45 Å) when compared to the idealized C–C distance in conjugated aromatic systems (cf. 1.38 Å in benzene), and the Pt–C1 distance is also relatively long (2.10 Å).^{10b,21} Intriguingly, the bond lengths of C2–C3 and C5–C6 are substantially shorter (1.35–1.38 Å) than those of C3–C4 and C4–C5 (1.39–1.42 Å), indicating partial location of the double bonds between C2–C3 and C5–C6, respectively. On the basis of these C–C and the regular C4–O bond distances, the positive charge in the cationic benzyl arenium systems can be tentatively located to a large extent on C4. These solid-state results strongly corroborate an arenium structure as deduced from NMR spectroscopy of these complexes in solution (vide supra) and deemphasize the relevance of π -complexes for these structures (cf. Figure 1). The presence of the phenolic proton (and therefore the absence of a ketone-type structure) in **5b** was confirmed indirectly. In the BF_4^- anion, one B–F bond is significantly longer than the others and points to the expected position of the phenolic hydrogen. Hence, hydrogen-bond-mediated self-assembly of the anion and the cation of **5b** occurs in the solid state. The large potential of the phenolic hydroxyl group in hydrogen bonding has some precedents from crystal engineering with related platinum(II) complexes containing functionalized pincer ligands.²⁹

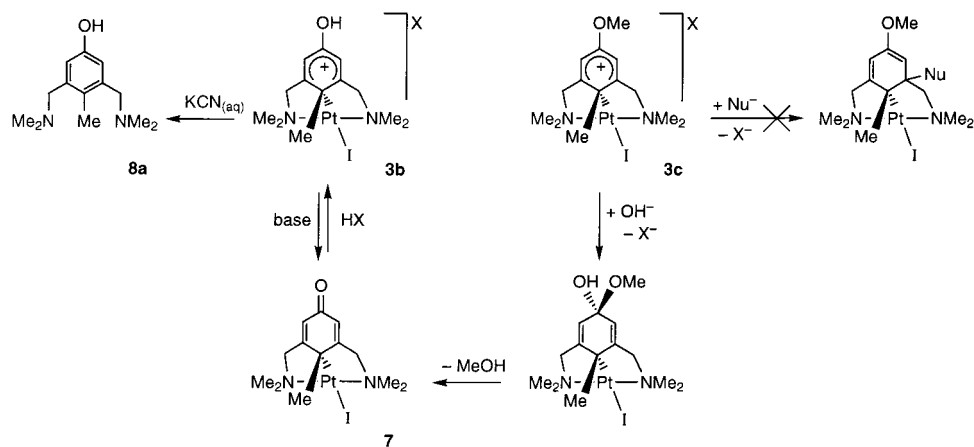
Reactivity toward Lewis Bases. Aqueous NaX solutions ($\text{X} = \text{Cl}, \text{Br}, \text{I}$) were shown previously to induce C–C bond cleavage in the platinum-stabilized arenium complex **3a** with concomitant re-aromatization, thus forming the neutral arylplatinum(II) complex **1a**.^{10b,c} Remarkably, the reactivity of arenium systems containing an oxo-functionality differs considerably. When the methyl arenium **3b** is dissolved in a minimum amount of THF and then treated with H_2O , an immediate color change from dark red to yellow is observed, irrespective of whether NaX salts are present or not. Toluene extraction gives a single organoplatinum complex **7** as a yellow solid, which exhibits the characteristic NMR-spectroscopic properties of 2,5-cyclohexadienones (Scheme 6).¹⁵ For example, the protons attached to the cyclohexadiene system give rise to a singlet at a field typical for olefinic protons ($\delta_{\text{H}} = 5.89$, toluene solution). Also, the ^{13}C NMR spectrum of **7** is in agreement with the presence of an α,β -unsaturated carbonyl system ($\delta_{\text{C}=\text{O}} = 186.3$, $\delta_{\text{C}} = 162.1$ and 119.6). Obviously, H_2O is a sufficiently strong base to abstract the proton, hence implying a pK_{a} of the phenolic proton in **3b** which is negative (cf. pK_{a} of H_3O^+). Complex **7** is also obtained quantitatively when the arenium **3b** is reacted with an organic base under anhydrous conditions (NEt_3 or NET^+Pr_2).

Surprisingly, an identical product **7** is formed exclusively, when the methoxy-substituted arenium **3c** is subjected to basic aqueous solutions. This may be explained by nucleophilic attack of OH^- ions at C4 of the arenium system, followed by cleavage of the in situ formed hemiketal and elimination of MeOH (Scheme 6). This hypothesis is strengthened by the results from experiments performed in ^{17}O -enriched H_2O . The ^{17}O NMR spectrum clearly reveals a broad signal at +450 ppm, which is

(28) (a) Olah, G. A.; Rasul, G. R.; Prakash, G. K. S. *J. Organomet. Chem.* **1996**, 521, 271. (b) Lambert, J. B.; Zhao, Y. *Angew. Chem.* **1997**, 109, 389; *Angew. Chem., Int. Ed. Engl.* **1997**, 36, 400. (c) Lambert, J. B.; Kania, L.; Zhang, S. *Chem. Rev.* **1995**, 95, 1191.

(29) (a) Albrecht, M.; Lutz, M.; Spek, A. L.; van Koten, G. *Nature* **2000**, 406, 970. (b) Braga, D.; Grepioni, F.; Desiraju, G. R. *Chem. Rev.* **1998**, 98, 1375.

Scheme 6



indicative for the presence of ^{17}O -labeled cyclic ketones.³⁰ The absence of any product arising from nucleophilic attack at C2 provides another (indirect) evidence for arenium systems in the complexes **3b–c**, which display a strong charge localization particularly on C4.¹⁵

In acidic environment, the ketone **7** was immediately protonated to give quantitatively arenium **3b** as was demonstrated by the typical red color of the product solution and by the pertinent NMR spectroscopic data. As assumed for such a ketone-to-enol transformation, the ^{17}O -labeled oxygen is more shielded in the enol situation, clearly reflected by a downfield shift of the ^{17}O NMR resonance to +300 ppm after addition of HBF_4 or HClO_4 to **7**. Hence, the transformation of arenium **3b** to the neutral platinum complex **7** is fully reversible.

Irreversible, however, are reactions with CN^- ions as nucleophiles, which lead to quantitative Pt–C bond cleavage and formation of an organic benzene derivative (Scheme 6). Platinum abstraction occurs presumably in the form of $[\text{Pt}(\text{CN})_4]^{2-}$ and corresponds to the last sequence of the aromatic substitution of a platinum substituent (formally PtX^+) by a carbocation (Me^+ , **8a**; Bn^+ , **8b**).

Identification of Intermediates Preceding Arenium Formation. The reactions of platinum *aqua* complexes with RX have been investigated in more detail by time-dependent spectroscopy. In particular, the reaction of **2b** with a large excess of BnBr in acetone is illustrative, since two sequential color changes have been observed (from colorless to purple and then to orange, *vide supra*). Monitoring of the arenium formation by in situ UV–vis spectroscopy provides valuable information on the course of the reaction. The initial color change from colorless to purple is reflected by the evolution of a broad absorption band located at 505 nm (purple solution, Figure 4a). The absorption band at this wavelength has reached its maximum 14 min after mixing of the reactants and subsequently starts to decrease. Simultaneously, a new absorption maximum at 430 nm is generated (orange solution, Figure 4b). The overlapping absorption spectra of this second color change clearly show the presence of an isosbestic point at 472 nm. Analysis of the time-dependent concentration of the purple intermediate, by its absorption at λ_{max} , has resulted in a reaction profile which is characteristic for sequential transformations of the type $\text{A} \rightarrow \text{B} \rightarrow \text{C}$ (Figure 5). The best theoretical approximation of the measured data points is based on rates for $k_{\text{B}} = 0.215 \text{ min}^{-1}$ and for $k_{\text{C}} = 0.0148 \text{ min}^{-1}$ (where k_{B} is

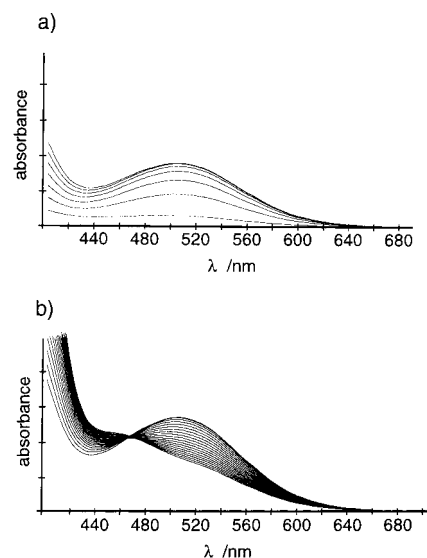


Figure 4. Overlapping absorption spectra (UV–vis spectroscopy, 2 min interval, acetone solution) showing the consecutive color changes (a) for the formation of the purple intermediate and (b) for the subsequent direct transformation to the orange arenium complex **5b**.

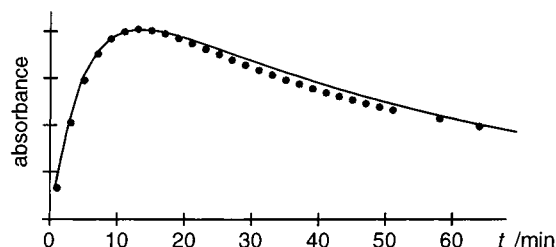


Figure 5. Time-dependent absorbance of the reaction solution (acetone) during the formation of **5b**, monitored at $\lambda = 505 \text{ nm}$, (λ_{max} of the purple intermediate). The solid line represents the calculated time-dependent concentration of the intermediate during a consecutive reaction from **2b** to **5b** (for reaction rates, see Table 2).

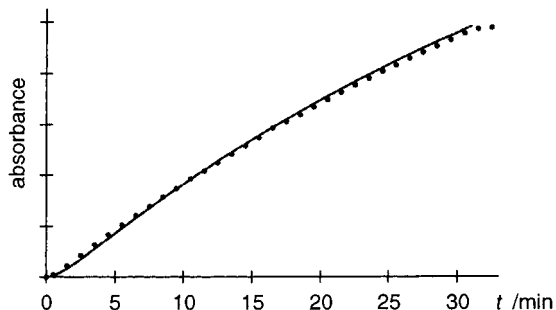
the observed rate constant for the formation of the intermediate and k_{C} the one for the formation of the arenium product). Qualitatively similar results have been obtained from measurements using BnBr and the methoxy-substituted *aqua* complex **2c** (Table 2).

No colored intermediates have been detected in the reaction of **2b** with MeI , and only the evolution of the dark red color of the arenium **3b** has been observed. The overlapping absorption spectra reveal a gradual, although not linear increase of the absorption band at $\lambda_{\text{max}} = 438 \text{ nm}$ without displaying any

(30) Kintzinger, J.-P. In *Oxygen-17 and Silicon-29 NMR, Basic Principles and Progress*; Diehl, P., Fluck, E., Kosfeld, R., Eds; Springer: Berlin, 1981; Vol. 17.

Table 2. Rate Constants for the Oxidative Addition (Formation of the (Alkyl)(Aryl) Platinum Species), and the Subsequent 1,2-Sigmatropic Shift (Arenium Formation)

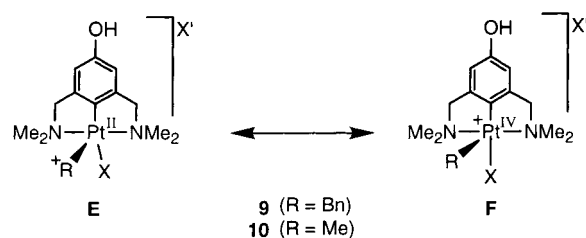
starting compounds	oxidative addition		sigmatropic shift	
	$k_{\text{obs}}/\text{min}^{-1}$	$\Delta G_{292}^{\ddagger}/\text{kJ mol}^{-1}$	$k_{\text{obs}}/\text{min}^{-1}$	$\Delta G_{292}^{\ddagger}/\text{kJ mol}^{-1}$
2b + MeI	0.980	10.0	0.0225	19.1
2b + BnBr	0.215	13.6	0.0148	20.1
2c + BnBr	0.305	12.8	0.0199	19.4

**Figure 6.** Time-dependent absorbance of the reaction solution (acetone) during the formation of **3b**, monitored at $\lambda = 438$ nm, (λ_{max} of the arenium complex **3b**). The solid line represents the calculated time-dependent concentration of **3b** formed by a consecutive reaction from **2b** via an intermediate (for reaction rates, see Table 2).

isosbestic point. The interpretation of the observed changes in absorbance (Figure 6) by means of sequential reaction kinetics affords an optimal correlation. This implies the postulation of a (not detected) intermediate, which has probably a structure similar to the one observed in the reaction of **2b** with BnBr (vide supra). Detailed analysis of the kinetic data reveals that the first step is dependent on both the alkyl group and the activating substituent on the aromatic system. The subsequent reaction of the intermediate to the arenium product is an order of magnitude slower and seems to be dominated by the nature of the alkyl group, since the activation energy ΔG^{\ddagger} for this process is smaller for benzyl groups than for methyl groups (Table 2).

Structural information on the purple intermediate has been obtained by in situ NMR spectroscopy of the reaction mixture. After addition of BnBr to a solution of **2b** (acetone- d_6), a significant broadening of the signal due to coordinated water is noted ($\delta_{\text{H}} = 2.85$; $\Delta w_{1/2} = 25$ Hz). After a few minutes, a set of signals appears which corresponds to the purple intermediate and which is characterized by diastereotopic NMe₂ ($\delta_{\text{H}} = 3.12$ and 2.83, respectively) and well-resolved CH₂N groups (AB doublet resonances at $\delta_{\text{H}} = 5.06$ and 3.58, $^2J_{\text{HH}} = 13.2$ Hz) resulting from a reduced symmetry in the intermediate complex. The signal due to the benzylic protons of the Bn group appears as a singlet at 4.61 ppm ($^2J_{\text{pH}} = 24$ Hz). A structure which is in full agreement with the observed spectroscopic data (NMR, UV-vis) comprises an (aryl)(alkyl) platinum complex containing the pincer ligand with an aryl unit that displays still aromatic character and a metal-bound alkyl group (benzyl in **9**, methyl in **10**; Figure 7).³¹

Two limiting resonance structures can be envisaged for these intermediates, comprising (i) a cationic alkyl group R (a Lewis acid), which is bonded to the nucleophilic and hence Lewis basic platinum(II) center (structure **E**, Figure 7),³² or (ii) a carbanion bound to an oxidized cationic platinum(IV) site as the product of an oxidative addition (structure **F**).³³ On the basis of the relatively small coupling constants of the benzylic protons of

**Figure 7.** Limiting resonance structures for the postulated (alkyl)(aryl) platinum complexes **9** and **10**, comprising a platinum(II) center and a cationic alkyl group (**E**), or an oxidized platinum(IV) center including a formally anionic alkyl ligand (**F**).

the Bn group in **9**, the notation of a platinum(IV) complex (i.e., **F**) is favored.³⁴ Moreover, the π -electron delocalization in the benzylic group is increased upon binding to platinum, which is in agreement with all spectroscopic properties of the observed intermediate (cf. the strong purple color of **9**). However, the postulated intermediates containing metal-bound ethyl or methyl groups such as **10** are expected to be colorless, as there is no π -electron delocalization along the alkyl fragment. Indeed these compounds are inactive in the diagnostic UV-vis region, and no intermediate was observed spectroscopically. Attempts to detect these intermediates by NMR spectroscopy also failed, probably because of a low effective concentration of **10** with respect to reactant and product (cf. Table 2), paired with a presumably large overlap of the characteristic resonance signals of the proposed intermediates and the formed arenium products.

Prolonged reaction time caused a gradual decrease of the set of signals assigned to **9** and concomitant formation of a new set of resonances, identical to the one of the final product **5b** (vide supra). The resonances of **9** do not disappear completely, however, because an equilibrium situation between complexes **9** and **5b** is reached (cf. isosbestic point in UV-vis spectra). The population of **5b** is strongly temperature-dependent and increases upon cooling. The benzylic protons of **5b** and **9** are diagnostic and were used to determine the equilibrium constant K (eq 1) at different temperatures. Following equations (1) and (2),

$$K = [\mathbf{5b}]/[\mathbf{9}] \quad (1)$$

$$\ln(K) = -\Delta G^{\circ}/RT = \Delta S^{\circ}/R - \Delta H^{\circ}/RT \quad (2)$$

the thermodynamic parameters were calculated as $\Delta H^{\circ} = -1.3$ (± 0.1) kJ mol⁻¹, $\Delta S^{\circ} = +3.8$ (± 0.2) J mol⁻¹K⁻¹ and ΔG°_{298}

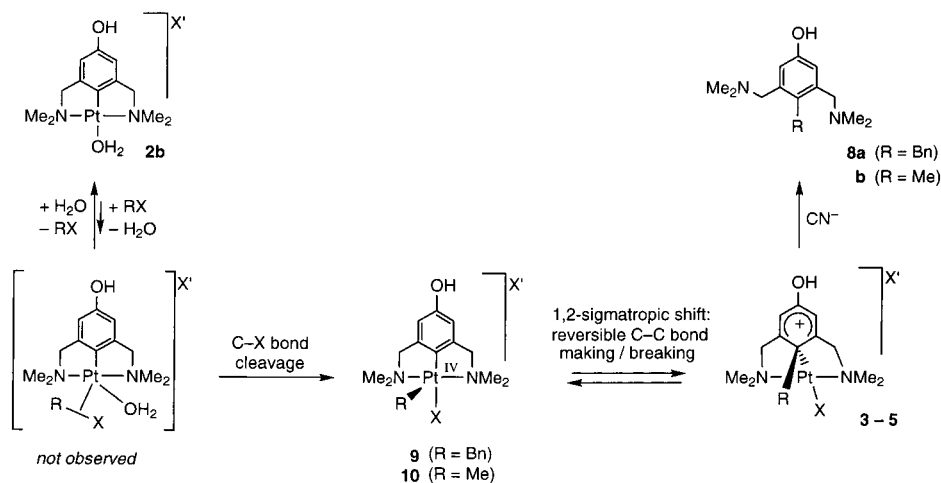
(32) The platinum center in complexes of the general type [PtX(NCN)] (X = halide) is a Lewis base, see, e.g.: (a) Reference 21b. (b) Muijsers, J. C.; Niemantsverdriet, J. W.; Wehman-Ooyevaar, I. C. M.; Grove, D. M.; van Koten, G. *Inorg. Chem.* **1992**, *31*, 2655.

(33) The relevance of similar resonance structures was also addressed in earlier studies on Pt(IV)⁺-H/Pt(II)-H⁺ (hydride vs proton) species, which showed that the actual structure is strongly determined by the nature of the extra (sixth) ligand *trans* to the Pt-H bond: (a) Wehman-Ooyevaar, I. C. M.; Grove, D. M.; Kooijman, H.; van der Sluis, P.; Spek, A. L.; van Koten, G. *J. Am. Chem. Soc.* **1992**, *114*, 9916. (b) Wehman-Ooyevaar, I. C. M.; Grove, D. M.; de Vaal, P.; Dedieu, A.; van Koten, G. *Inorg. Chem.* **1992**, *31*, 5484. Note the related discussion concerning the catalytic cycle in Pd-mediated Heck chemistry, especially with respect to the existence of Pd(IV) intermediates, which may or may not be involved, see, e.g.: (c) Mitchell, T. N. In *Metal-Catalyzed Cross-coupling Reactions*; Diederich, F., Stang, P. J., Eds.; Wiley-VCH: Weinheim, 1998; p 167. (d) Reetz, M. T.; Westermann, E. *Angew. Chem.* **2000**, *112*, 170; *Angew. Chem., Int. Ed.* **2000**, *39*, 165. (e) Shaw, B. L. *New J. Chem.* **1998**, *77*. (f) Ohff, M.; Ohff, A.; van der Boom, M. E.; Milstein, D. *J. Am. Chem. Soc.* **1997**, *119*, 11687. (g) Amatore, C.; Jutland, A. *Acc. Chem. Res.* **2000**, *33*, 314. (h) Beletskaya, I. P.; Cheprakov, A. V. *Chem. Rev.* **2000**, *100*, 3009.

(34) Terheijden, J.; van Koten, G.; de Booys, J. L.; Ubbels, H. J. C.; Stam, C. H. *Organometallics* **1983**, *2*, 1882.

(31) Vignalok, A.; Rybtchinski, B.; Shimon, L. J. W.; Ben-David, Y.; Milstein, D. *Organometallics* **1999**, *18*, 895.

Scheme 7



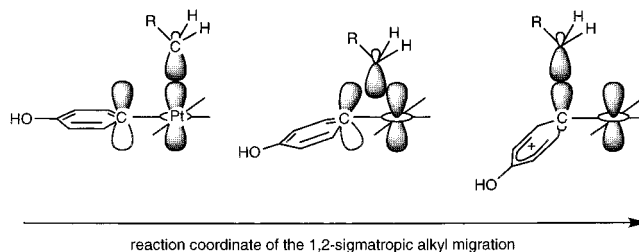
$= -2.4 (\pm 0.1) \text{ kJ mol}^{-1}$. Note the small entropy factor, which is typical for intramolecular processes. Remarkably, no indication was found for a similar equilibrium during the migration of the methyl group from **10** to form **3b**, presumably owing to a higher stability of the arenium product relative to the (alkyl)-(aryl) platinum intermediate, that is ΔG° is much larger than for the products from a reversible 1,2-shift of the benzyl group from **5b** to **9** along the Pt–C bond.

Discussion

So far, accessibility of metal-stabilized arenium complexes and hence the formation of a new C–C bond in Pt(NCN) and related complexes has been restricted to methyl arenium ions. Only recently, stable ethyl and benzyl analogues have been reported.^{20,31} The introduction of electron-releasing groups as activators on the aromatic ring broadens the scope of this reaction significantly and provides access to various arenium systems containing, for example, ethyl, benzyl, or silyl groups. This identifies the arenium formation as a general process in metal-catalyzed $\text{C}_{\text{aryl}}\text{--C}_{\text{alkyl}}$ bond making and breaking, similar to Friedel–Crafts alkylations.³⁵ Full control on such species is therefore highly desirable and requires (i) accessibility and stabilization (e.g., isolation) of arenium intermediates and (ii) the ability to tune their reactivity, thus determining the further reaction profile and hence product selectivity (Scheme 1).

Controlling the Arenium Formation. Activation of the Alkyl halide (RX). The fact that the platinum complex **2a** is prone to form selectively arenium ions with MeX suggested an $\text{S}_{\text{N}}2$ -type reaction at the halide-bound carbon. For these reactions, a high sensitivity of the reaction rate to steric bulk at the carbon atom is expected, and this is confirmed by the reactivity of the activated platinum complexes **2b–d** toward various RX (MeX > BnX > EtX). No arenium product at all has been observed when aryl halides PhX or secondary or tertiary alkyl halides such as ^iPrX or ^tBuX have been used. These latter results are expected in $\text{S}_{\text{N}}2$ -type nucleophilic substitutions, since highly branched alkyl halides are known to follow almost exclusively ionic pathways via prior heterolytic C–X bond cleavage ($\text{S}_{\text{N}}1$ -type reactions).³⁶ Aryl halides, in contrast, generally do not follow nucleophilic substitution pathways, irrespective of whether

Scheme 8



they contain electron-withdrawing or -releasing substituents. Moreover, in all the experiments leading to arenium formation, the halide X behaves as a classical leaving group (cf. the faster rate of the reaction of **2b** with BnBr compared to that of the reaction with BnCl), thus supporting a nucleophilic substitution reaction as initial step of arenium formation (Scheme 7). Owing to the orbital situation on the metal center in **2** (d_{z^2} empty, d_{xz} filled), the nucleophilic attack of the platinum center most presumably occurs “side-on” (Scheme 7) and not in a classical conformation with the leaving group and the nucleophile in the two apical positions of a trigonal bipyramidal carbon center.^{10d} This yields an (alkyl)(aryl) platinum complex (e.g. **9**, **10** in Scheme 7) as an intermediate, which may or may not contain a coordinated solvent molecule (H_2O).

Reversible 1,2-Shift of the Organic Ligand R along the Pt–C Bond. Arenium formation is completed by a second reaction sequence, that is, a 1,2-sigmatropic shift of the metal-bound alkyl group to the aromatic carbon (Scheme 7). This is equal to the intimate step of reversible C–C bond making and breaking. The isosbestic point observed in the overlapping UV–vis spectra of this reaction indicates an equilibrium situation and hence a reversible process. In addition, the isosbestic point excludes any intermediate during this reaction (on the UV–vis time scale), which identifies this sigmatropic shift as a *direct* transformation of a C–C bond cleaved species to a C–C bond formed product and vice versa. Formally, the migrating species is a carbocation (a metal-generated electrophile), which reacts in a highly regioselective electrophilic substitution reaction with the aromatic system of the pincer ligand (Scheme 8). The cationic nature of the migrating group is essential to ensure conservation of orbital symmetry³⁷ and was explained by hybridization of the metal-centered d_{z^2} (empty in a d^6 Pt(IV) complex) with a filled p_z orbital (hybridization not shown in

(35) Taylor, R. *Electrophilic Aromatic Substitution*; Wiley: New York, 1990.

(36) The observed products resulting from Pt–C bond cleavage may be a consequence of the oxidizing environment due to released I^- . A cascade of oxidative addition and reductive elimination cycles may then afford inorganic salts such as $[\text{PtI}_4]^{2-}$ along with noncoordinating pincer ligand.

(37) Woodward, R. B.; Hoffmann, R. *The Conservation of Orbital Symmetry*; VCH: Weinheim, 1970.

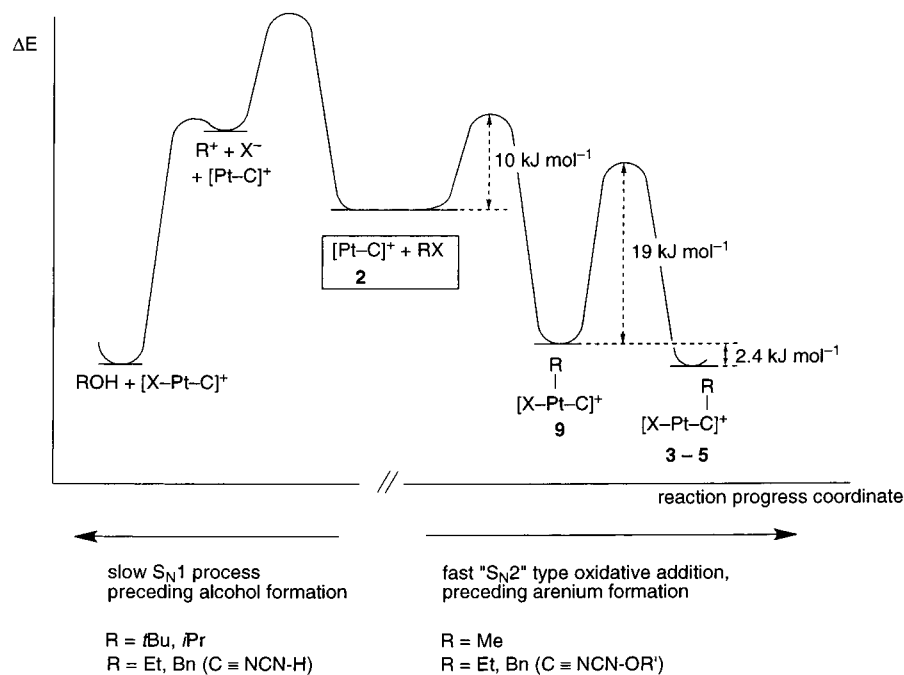


Figure 8. Energy profile of the reaction progress coordinate of the reaction of the platinum *aqua* complex **2** with an alkyl halide RX to form either a new C–C bond or the corresponding alcohol ROH (energy values belong to the reaction of **2b** with BnBr and are taken from Table 2 (ΔG^\ddagger) and from temperature-dependent NMR experiments (ΔG°), vide supra). Notably, for the reaction of **2a** (lacking aromatic oxo-substituents) with RX ($R \neq \text{Me}$), the activation energy for the 1,2-sigmatropic shift is much higher than 19 kJ mol^{-1} and consequently, the reaction trajectory toward the formation of ROH is a slow but favored process.

Scheme 8) during the sigmatropic shift process.^{10d} Tilting of the phenyl ring with respect to the Pt–C_{ipso} bond presumably occurs synchronously with the 1,2-sigmatropic migration of the alkyl group, similar to the established process for, for example, the pinacol rearrangement. Owing to the resonance-stabilization in benzyl groups, the transition state of the sigmatropic shift (Scheme 8) is expected to be more easily accessible with Bn⁺ than with Me⁺ ions, which is also reflected in the corresponding rates of this migration process (Table 2).

These results provide for the first time direct evidence for a *reversible migration of a benzyl cation along a metal–carbon bond*: the spectroscopic observations visualize the reaction trajectory for a reductive elimination process (i.e., C_{arenium}–C_{alkyl} bond formation) taking place at a platinum center, and in particular, also demonstrate the microscopic reverse, that is that for a metal-mediated C–C bond activation and cleavage process. In either reaction direction, the formation of the arenium ion is crucial. Notably, these findings seem to contrast with *P,C,P*-terdentate coordinating PCP-pincer complexes with Rh(I), which were shown to mediate both C_{aryl}–C_{alkyl} and C_{alkyl}–H bond cleavage.³⁸ With these systems, arenium complexes such as **3–5** are less easily accessible than with platinum. Theoretical considerations predict that, irrespective of the substituents on the phosphine donors, a π -complex is an initial intermediate of the C–C bond activation process. Ab initio calculations have emphasized the relevance of agostic C_{aryl}–C_{alkyl} interactions, and such structures have indeed been isolated and proposed as arrested intermediates. Although similar agostic bonding has not been observed in Pt(NCN)-type complexes thus far, it is noteworthy that the transition state of the 1,2-sigmatropic shift possesses a strongly related geometry (Scheme 8, Figure 8). Obviously, the different electronic configuration of the rhodium and platinum center in these complexes (oxidation

state, d⁶ vs d,⁸ PCP vs NCN ligand skeleton) directs whether agostic structure and arenium complexes are intermediates or transition states in metal-mediated C–C bond making and breaking.

Activated Aromatic Systems. According to the reactivity of the platinum *solvato* complexes **2a–d**, the presence of electron-releasing oxo-substituents on the aromatic ring of the pincer ligand affects the formation of alkyl arenium ions significantly. Such substituents are known to activate the aromatic system and also to stabilize the positive charge in the arenium product. These influences are particularly well-documented in electrophilic aromatic substitution theory.⁴

This analogy to electrophilic aromatic substitution provides also a rationale for the earlier observed formation of ROH and a zwitterionic platinum dimer, when **2a** is exposed to alkyl halides RX (where $R \neq \text{Me}$, vide supra). Notably, this process is very slow and therefore was attributed to a secondary reaction pathway which becomes obviously competitive when the primary, much faster process (arenium formation) is disfavored. This may be caused either by a too large activation energy for the formation of the (alkyl)(aryl) platinum complex or for the arenium product (Figure 8). In particular, the 1,2-sigmatropic shift leading to arenium complexes is expected to be very sensitively tuned by the electronic properties of the aryl unit. In the absence of activating oxo-substituents (cf. **2a**), the energy barrier for the 1,2-sigmatropic migration is probably too high, and instead, the backward reaction becomes important, that is, reductive elimination of RX from the (alkyl)(aryl) platinum complex and irreversible formation of ROH. Formation of ROH is most likely a metal-mediated process comprising solvent coordination on the (alkyl)(aryl) platinum(IV) species to give an octahedral d⁶ complex. Reductive elimination is accompanied by the release of one equivalent of H⁺, which slowly protonates the nitrogen donor sites of the pincer ligand, thus ultimately leading to the zwitterionic dimeric complex as depicted in Scheme 2.

(38) (a) Sundermann, A.; Uzan, O.; Milstein, D.; Martin, J. M. J. *J. Am. Chem. Soc.* **2000**, *122*, 7095. (b) Rybtchinski, B.; Vignalok, A.; Ben-David, Y.; Milstein, D. *J. Am. Chem. Soc.* **1996**, *118*, 12406.

Controlling the Reactivity of Arenium Ions. Trapping the Arenium Intermediate by Nucleophiles: Addition Reaction.

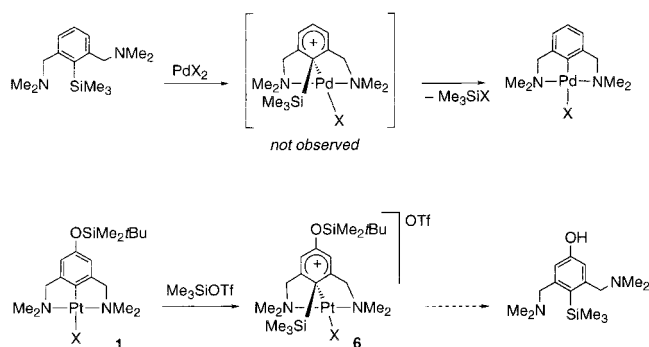
For the oxo-substituted arenium species **3b**, **3c**, **4**, and **5**, an α,β -unsaturated ketone-type structure has been deduced (vide supra). Therefore, the reactivity of these complexes was probed with various nucleophiles to form the corresponding neutral cyclohexadiene-type addition products. In contrast to the established reactivity of **3a** (lacking an oxo-substituent on the arenium moiety), all of the used nucleophiles undergo selective 1,4-disubstitution, leading to cyclohexa-2,5-diene products exclusively (Scheme 6). No 1,2-disubstituted cyclohexa-2,4-diene products (Scheme 1) were detected.¹⁵ The hydroxyl-substituted arenium ions undergo a proton abstraction reaction rather than a nucleophilic substitution, mediated by organic (NEt₃) or weak inorganic bases (H₂O), thus forming a cyclohexa-2,5-dien-4-one product. Interestingly, nucleophilic attack by H₂O may occur either at the phenolic proton of **3b**, or on the oxygen-bound carbon, thus initially producing a geminal diol, which subsequently dehydrates spontaneously (cf. Scheme 6).

Completion of C–C Bond Formation: Formal Substitution of [PtX]⁺ by [R]⁺. The substitution reaction was completed by addition of CN[−] ions, which induced irreversible Pt–C bond cleavage in the arenium ions **3–5** (Scheme 7). The platinum fragment was probably released as an inorganic salt, for example, [Pt(CN)₄]^{2−}, with concomitant re-aromatization of the aryl system. The *full* microscopic reverse of this C–C bond formation process, that is the cleavage of a tolyl C_{aryl}–C_{alkyl} bond in **8** to form **2** is not accessible so far in NCN pincer chemistry, but ample evidence for this reaction has been given by using corresponding PCP pincer-type ligands instead of NCN.^{3e,19,31} This difference in reactivity presumably originates from the different M–L bond strength of metals to amines and phosphines, which is stronger for the latter (L = PR₃) compared to amines (L = NR₃). Therefore, replacement of a ligand in the metal precursor, which is in this case essential for subsequent C–C bond activation and cleavage, is generally achieved by phosphine ligands but not by amines.^{10a,14d}

Silylated Arenium Complexes: Intermediates in Transmetalation Reactions. The color and especially the chemical shift values from ²⁹Si NMR of the complex **6a** provide good evidence for the presence of a silylated arenium complex. Alternative structures comprising either silicenium ions, Me₃Si⁺, or siloxonium ions, (R₃Si)₂OR⁺, may be excluded.^{23a,28,39} This is particularly relevant in the context of recent (trans)palladation studies using silylated NCN pincer ligands.

Selective C_{aryl}–Si bond cleavage is a key step in this protocol and has been tentatively proposed to be induced by an electrophilic attack of the palladium precursor, thus affording a (unstable) silylated arenium intermediate (Scheme 9).⁴⁰ Unfortunately, the high reaction rate of these sequences (presumably second-order in nucleophile) and also of the subsequent re-aromatization step (comprising the loss of Me₃Si⁺) precludes experimental verification of this mechanistic proposal. The platinum silyl arenium **6a** represents a frozen intermediate of this process and identifies the transpalladation sequence as an electrophilic aromatic substitution of the Me₃Si⁺ fragment by a PdL⁺ moiety. This points to a mechanism

Scheme 9



for this palladation reaction which is the microscopic reverse of the formation of the silyl arenium **6a** and related alkyl arenium ions and hence involves as a key step the electrophilic aromatic substitution of the silyl substituent Me₃Si⁺ by a palladium unit PdL⁺.⁴¹ Similarly, metal-mediated C_{aryl}–H bond activation is assumed to follow a similar reaction trajectory as outlined in Figure 8 (with R = H).

Conclusions

Platinum-mediated sp²–sp³ C–C bond formation between an aryl carbon of the NCN pincer ligand alkyl halides RX have been established for various alkyl groups (R = methyl, ethyl, benzyl). Essential for the occurrence of these processes is the presence of activating substituents on the aromatic system of the platinum-bound NCN pincer ligand such as electron-releasing OH or OR groups. Application of this principle allowed furthermore for the preparation and identification of silyl arenium ions without using a superacidic environment. Apart from the activating effect, the aromatic oxo-substituents also stabilize important intermediates. This provided direct evidence for the intimate steps of this carbon–carbon bond formation process, which involves first oxidative addition of RX to the platinum center and formation of an (alkyl)(aryl) metal complex. A reversible 1,2-sigmatropic shift of the alkyl group along the platinum–carbon bond subsequently generates the arenium product. Strong similarities between the reaction trajectory of metal-mediated C–C bond making and breaking and the electrophilic aromatic substitution reaction (Friedel–Crafts alkylation) have been established, including: (i) the electrophilic mode of action of the metal center in activating the alkyl halide; (ii) the increase of reactivity of the arene unit upon substitution with electron-releasing substituents (such as OR); (iii) electrophilic attack of the alkyl cation on the arene system with a reactivity sequence Et < Bn < Me. In both processes, control on the stability and reactivity of the arenium intermediate is crucial for determining the outcome of the reaction, that is, C–C bond formation, cleavage or nucleophilic addition (cyclohexadiene formation). Consideration of these fundamental principles is expected to provide access to an improved understanding of the essential parameters for the design of efficient catalysts for C_{aryl}–C_{alkyl} bond activation or cleavage.

Experimental Section

General. Syntheses involving air-sensitive reagents (organolithium species, Me₃SiOTf) were carried out under a dry nitrogen atmosphere using Schlenk techniques and freshly distilled solvents (CH₂Cl₂ from

(39) (a) Olah, G. A.; Rasul, G.; Prakash, G. K. S. *J. Am. Chem. Soc.* **1999**, *121*, 9615. (b) Lambert, J. B.; Zhang, S.; Stern, C. L.; Huffman, J. C. *Science* **1993**, *260*, 1917.

(40) (a) Valk, J.-M.; Boersma, J.; van Koten, G. *J. Organomet. Chem.* **1994**, *483*, 213. (b) Steenwinkel, P.; Gossage, R. A.; van Koten, G. *Chem. Eur. J.* **1998**, *5*, 759. (c) Steenwinkel, P.; Gossage, R. A.; Maunula, T.; Grove, D. M.; van Koten, G. *Chem. Eur. J.* **1998**, *5*, 763.

(41) For a similar arenium intermediate as a snapshot during a transmetalation reaction, see: Abbenhuis, H. C. L.; Feiken, N.; Haarman, H. F.; Grove, D. M.; Horn, E.; Kooijman, H.; Spek, A. L.; van Koten, G. *Angew. Chem.* **1991**, *103*, 1046; *Angew. Chem., Int. Ed. Engl.* **1991**, *30*, 996.

CaH₂, pentane from Na/benzoketyl). All NMR spectra (δ in ppm; J in Hz; ¹H at 300 MHz, ¹³C {¹H} at 75 MHz, ¹⁷O at 54.2 MHz, and ²⁹Si {¹H} NMR at 59.6 MHz) were recorded at room temperature, unless stated otherwise, and referenced to SiMe₄ (¹H, ¹³C, and ²⁹Si) or residual H₂O (δ = 0.0 ppm; ¹⁷O). All assignments in ¹H and ¹³C NMR are based either on distortionless enhancement of polarization transfer (DEPT) experiments or on heteronuclear shift correlation spectroscopy. UV-vis photospectroscopy was carried out on a Cary1 spectrophotometer at room temperature. Elemental analyses were performed by Kolbe, Mikroanalytisches Laboratorium, Mülheim/Ruhr. The platinum complexes **1a**,^{10b} **1b**,^{27a} **1d**,^{21b} **2a**,^{10b} **3a**,^{10b} and the ligand precursor NC-(Br)N-OMe⁴² were prepared according to literature procedures.

[PtCl(C₆H₂{CH₂NMe₂}₂-2,6-OMe-4)] (1c). To a cooled (−78 °C) solution of C₆H₃-Br-1-{CH₂NMe₂}₂-2,6-OMe-4 (1.21 g, 4.0 mmol) in hexane (15 mL) was added a solution of ^tBuLi (5.3 mL, 7.9 mmol, 1.5 M in hexane). The reaction solution was allowed to warm to room temperature within 12 h. After removal of all volatiles in vacuo, the yellowish residue was redissolved in Et₂O (20 mL). To this solution was added solid [PtCl₂(SEt₂)₂] (1.78 g, 4.0 mmol), and stirring was continued for 12 h. Solid LiBr (0.87 g, 10 mmol) was added and the mixture stirred another 12 h. All volatiles were evaporated in vacuo and the residue suspended in pentane. The precipitated was collected by centrifugation and washed with portions of pentane (2 × 30 mL). Consecutive extraction of the solid with CH₂Cl₂ afforded 1.75 g (3.5 mmol) of the bromide analogue of **1c**, which has been redissolved in wet acetone (10 mL, acetone/H₂O 10:1). After treatment with AgOTf (0.91 g, 3.5 mmol) in the absence of light for 30 min and subsequent filtration through Celite, a colorless solution was obtained. A solution of NaCl (0.88 g, 15 mmol in 6 mL H₂O) was added and the suspension stirred vigorously for 2 h. The precipitate was collected and recrystallized from CH₂Cl₂ and pentane to yield analytically pure **1c** (1.52 g, 84%). ¹H NMR (CDCl₃): δ = 6.45 (s, 2H, C₆H₂), 3.99 (s, 4H, ³J_{PH} = 45.9 Hz, CH₂N), 3.73 (s, 3H, OCH₃), 3.07 (s, 12H, ³J_{PH} = 37.5 Hz, NCH₃); ¹³C {¹H} NMR (CDCl₃): δ = 157.4 (C_{para}), 143.8 (C_{ortho}), 135.7 (C_{ipso}), 105.7 (C_{meta}), 77.8 (²J_{PTC} = 66 Hz, CH₂N), 55.6 (OCH₃), 54.4 (²J_{PTC} = 18 Hz, NCH₃); Anal. Calcd for C₁₃H₂₁ClN₂O₂Pt (451.87): C, 34.56; H, 4.68; N, 6.20. Found: C, 34.41; H, 4.69; N, 6.16.

[Pt(C₆H₂{CH₂NMe₂}₂-2,6-OH-4)(OH₂)X] (2b, X = BF₄ or CF₃SO₃). To a suspension of [PtCl(C₆H₂{CH₂NMe₂}₂-2,6-OH-4)] (**1b**, 97 mg, 0.22 mmol) in acetone/H₂O (3 mL, 10:1) was added solid AgCF₃SO₃ (57 mg, 0.22 mmol) or AgBF₄ (43 mg, 0.22 mmol). The mixture was stirred while protected from light at room temperature for 30 min. The suspension was filtered through Celite under nitrogen while protected from light to yield a colorless filtrate. The solvent was removed from the filtrate in vacuo to leave the title product as a colorless solid. Analysis for X = SO₃CF₃: yield 110 mg, 84%. ¹H NMR (acetone-*d*₆): δ = 7.90 (s, 1H, Ar-OH), 6.45 (s, 2H, ⁴J_{PH} = 8.9 Hz, C₆H₂), 4.12 (s, 4H, ³J_{PH} = 50.5 Hz, CH₂N), 3.01 (s, 12H, ³J_{PH} = 33.0 Hz, NCH₃), 2.6–3.1 (br s, 2H, H₂O); ¹³C {¹H} NMR (acetone-*d*₆): δ = 156.8 (C_{para}), 145.2 (²J_{PTC} not resolved, C_{ortho}), 108.1 (³J_{PTC} = 42.7 Hz, C_{meta}), 76.6 (²J_{PTC} = 70.9 Hz, CH₂N), 54.1 (²J_{PTC} = 19.6 Hz, NCH₃), C_{ipso} not observed; Anal. Calcd for C₁₃H₂₁F₃N₂O₅PtS (569.47): C, 27.42; H, 3.72; N, 4.92. Found: C, 27.58; H, 3.68; N, 4.96. Analysis for X = BF₄ (recrystallized from THF at −20 °C): Yield 108 mg (96%). ¹H NMR (acetone-*d*₆): δ = 7.99 (s, 1H, Ar-OH), 6.47 (s, 2H, ⁴J_{PH} = 9 Hz, C₆H₂), 4.17 (s, 4H, ³J_{PH} = 51.6 Hz, CH₂N), 2.99 (s, 12H, ³J_{PH} = 37.8 Hz, NCH₃), 2.83 (br s, 2H, H₂O); ¹³C {¹H} NMR (acetone-*d*₆): δ = 156.7 (C_{para}), 145.1 (²J_{PTC} not resolved, C_{ortho}), 108.2 (³J_{PTC} = 40 Hz, C_{meta}), 76.6 (²J_{PTC} = 72 Hz, CH₂N), 54.3 (²J_{PTC} = not resolved, NCH₃), C_{ipso} not observed; Anal. Calcd for C₁₂H₂₁BF₄N₂O₂Pt × 0.5 THF (543.26): C, 30.95; H, 4.64; N, 5.16. Found: C, 30.55; H, 5.08; N, 5.34.

[Pt(C₆H₂{CH₂NMe₂}₂-2,6-OMe-4)(OH₂)] [CF₃SO₃] (2c). The procedure was analogous to the preparation of **2b**. Reaction of **1c** (0.90 g, 2.0 mmol) with AgCF₃SO₃ (0.51 g, 2.0 mmol) in acetone/H₂O (5 mL, 10:1) yielded, after filtration through Celite, **2c** as a white solid (1.01 g, 87%). Analytically pure **2c** was obtained by recrystallization from THF at −20 °C. ¹H NMR (acetone-*d*₆): δ = 6.54 (s, 2H, C₆H₂), 4.19

(s, 4H, ³J_{PH} = 49.6 Hz, CH₂N), 3.73 (s, 3H, OCH₃), 3.02 (s, 12H, ³J_{PH} = 36.6 Hz, NCH₃), 2.8 (br s, 2H, H₂O); Anal. Calcd for C₁₃H₂₃-BF₄N₂O₂Pt (521.23): C, 29.96; H, 4.45; N, 5.37. Found: C, 30.01; H, 4.46; N, 5.19.

[Pt(C₆H₂{CH₂NMe₂}₂-2,6-OSiMe₂-Bu-4)(OH₂)] [CF₃SO₃] (2d). The procedure was analogous to the one described for **2b**, starting from **1d** (1.17 g, 2.1 mmol) and AgCF₃SO₃ (0.55 g, 2.1 mmol) in acetone/H₂O (10 mL, 10:1) Filtration off the precipitate formed after 30 min (Celite) and concentration of the filtrate to ca. 1 mL followed by layering with Et₂O gave colorless crystals of **2d** (Yield: 1.01 g, 87%). ¹H NMR (acetone-*d*₆): δ = 6.47 (s, 2H, C₆H₂), 4.16 (s, 4H, ³J_{PH} = 50.4 Hz, CH₂N), 3.01 (s, 12H, ³J_{PH} = 37.5 Hz, NCH₃), 2.82 (br s, 2H, OH₂), 0.98 (s, 9H, CCH₃), 0.18 (s, 6H, SiCH₃); ¹³C {¹H} NMR (acetone-*d*₆): δ = 154.8 (C_{para}), 145.3 (C_{ortho}), 112.6 (³J_{PTC} = 43.5 Hz, C_{meta}), 76.5 (²J_{PTC} = 72.0 Hz, CH₂N), 54.1 (²J_{PTC} = 17.0 Hz, NCH₃), 26.0 (CCH₃), 18.3 (SiCCH₃), −4.3 (SiCH₃), C_{ipso} not observed; Anal. Calcd for C₁₉H₃₅F₃N₂O₅PtSSi (683.74): C, 33.38; H, 5.16; N, 4.10. Found: C, 33.37; H, 5.10; N, 4.13.

[Pt(C₆H₂{Me}-1-{CH₂NMe₂}₂-2,6-OH-4)] [CF₃SO₃] (3b). To a solution of **2b** (98 mg, 0.17 mmol) in acetone (3 mL) was added excess MeI (1 mL, 16 mmol). Stirring was continued for 24 h during which time the initially colorless solution slowly turned dark red. Evaporation of all volatiles in vacuo afforded analytically pure **3b** as a red solid (119 mg, 100%). ¹H NMR (acetone-*d*₆): δ = 7.07 (s, 2H, C₆H₂), 4.94 (d, 2H, ²J_{HH} = 13.4 Hz, ³J_{PH} = 29.4 Hz, CH₂N, lowfield part of ABq), 3.63 (d, 2H, ²J_{HH} = 13.7 Hz, ³J_{PH} = 38.6 Hz, CH₂N, highfield part of ABq), 3.14 (s, 6H, ³J_{PH} = 36.1 Hz, NCH₃Me), 2.82 (s, 6H, ³J_{PH} = 31.3 Hz, NMeCH₃), 2.70 (s, 3H, CCH₃); ¹³C {¹H} NMR (acetone-*d*₆): δ = 172.1 (C_{para}), 155.7 (²J_{PTC} = 27.8 Hz, C_{ortho}), 117.4 (³J_{PTC} = 33.2 Hz, C_{meta}), 80.4 (¹J_{PTC} not resolved, C_{ipso}), 68.9 (²J_{PTC} = 47.2 Hz, CH₂N), 58.0 (²J_{PTC} not resolved, NCH₃Me), 55.1 (²J_{PTC} = 19.1 Hz, NMeCH₃), 19.2 (²J_{PTC} not resolved, CCH₃); ¹⁷O NMR (THF): δ = 300; Anal. Calcd for C₁₄H₂₂F₃IN₂O₄PtS (693.39): C, 24.25; H, 3.20; N, 4.04. Found: C, 24.16; H, 3.26; N, 4.02.

[Pt(C₆H₂{Me}-1-{CH₂NMe₂}₂-2,6-OMe-4)] [CF₃SO₃] (3c). To a solution of **2c** (1.17 g, 2.0 mmol) in acetone (8 mL) was added excess MeI (2 mL, 32 mmol). The initially colorless solution slowly turned red. After 20 h, the solution was evaporated to dryness, and the residue was redissolved in CH₂Cl₂ (3 mL). This solution was overlaid with pentane (15 mL) to afford red crystals of **3c** (1.33 g, 94%). ¹H NMR (acetone-*d*₆): δ = 7.28 (s, 2H, C₆H₂), 5.01 (d, 2H, ²J_{HH} = 13.2 Hz, ³J_{PH} = 25.4 Hz, CH₂N, lowfield part of ABq), 4.21 (s, 3H, OCH₃), 3.77 (d, 2H, ²J_{HH} = 13.2 Hz, ³J_{PH} = 41.0 Hz, CH₂N, highfield part of ABq), 3.15 (s, 6H, ³J_{PH} = 36.1 Hz, NCH₃Me), 2.84 (s, 3H, ³J_{PH} = 30.4 Hz, CCH₃), 2.81 (s, 6H, ³J_{PH} = 30.4 Hz, NMeCH₃); ¹³C {¹H} NMR (acetone-*d*₆): δ = 171.0 (C_{para}), 152.2 (²J_{PTC} = 25.1 Hz, C_{ortho}), 116.2 (³J_{PTC} = 38.2 Hz, C_{meta}), 84.8 (¹J_{PTC} = 1100 Hz, C_{ipso}), 68.8 (²J_{PTC} = 51.1 Hz, CH₂N), 58.8 (OCH₃), 58.3 (²J_{PTC} = 13.1 Hz, NCH₃Me), 55.1 (²J_{PTC} = 16.9 Hz, NMeCH₃), 18.9 (²J_{PTC} = 75.2 Hz, CCH₃); Anal. Calcd for C₁₅H₂₄F₃IN₂O₄PtS (707.42): C, 25.47; H, 3.42; N, 3.96. Found: C, 25.35; H, 3.35; N, 3.84.

Synthesis of [Pt(C₆H₂{Et}-1-{CH₂NMe₂}₂-2,6-OH-4)] [BF₄] (4a). To a stirred solution of **2b** (0.63 g, 1.24 mmol) in acetone (15 mL) was poured excess EtI (5 mL, 60 mmol). After stirring over 16 h, the solution had become dark red, and a white precipitate had formed. The precipitate was removed by filtration (Celite), and the filtrate was evaporated to dryness. The crude product was dissolved in CH₂Cl₂ (5 mL) and precipitated with pentane (50 mL). Repetition of this procedure afforded **4a** as a red oily solid (0.32 g, 40%). ¹H NMR (acetone-*d*₆): δ = 7.12 (s, 2H, C₆H₂), 4.94 (d, 2H, ²J_{HH} = 13.2 Hz, CH₂N, lowfield part of ABq), 3.58 (d, 2H, ²J_{HH} = 13.7 Hz, CH₂N, highfield part of ABq), 3.53 (q, 2H, ³J_{HH} = 7.2 Hz, CCH₂CH₃), 3.12 (s, 6H, ³J_{PH} = 36.0 Hz, NCH₃Me), 2.81 (s, 6H, ³J_{PH} = 28.5 Hz, NMeCH₃), 0.64 (t, 3H, ³J_{HH} = 7.2 Hz, CCH₂CH₃); ¹³C {¹H} NMR (acetone-*d*₆): δ = 173.2 (C_{para}), 156.5 (C_{ortho}), 119.0 (C_{meta}), 86.4 (C_{ipso}), 69.0 (CH₂N), 58.1 (NCH₃Me), 55.4 (NMeCH₃), 28.9 (CCH₂CH₃), 16.0 (CCH₂CH₃); Anal. Calcd for C₁₄H₂₄BF₄IN₂O₂Pt (645.15): C, 26.06; H, 3.75; N, 4.34. Found: C, 25.89; H, 3.82; N, 4.25.

[PtBr(C₆H₂{Et}-1-{CH₂NMe₂}₂-2,6-OH-4)] [BF₄] (4b). The procedure was analogous to the preparation of **4a**, starting from **2b** (0.63 g, 1.24 mmol) in acetone (15 mL) and EtBr (5 mL, 70 mmol). After

(42) van de Kuil, L. A.; Luitjes, J.; Grove, D. M.; Zwikker, J. W.; van der Linden, J. G. M.; Roelofsen, A. M.; Jenneskens, L. W.; Drenth, W.; van Koten, G. *Organometallics* **1994**, *13*, 468.

stirring over 24 h, the formed suspension was filtered (Celite) and the red filtrate was evaporated to dryness. Analysis of the crude product showed ca. 50% unreacted **2c**. Acetone (10 mL) and additional EtBr (5 mL) were added, and the reaction was left for 7 days, during which again a precipitate formed. This was removed and the residual solution treated with pentane. Repeated dissolving in CH₂Cl₂ (5 mL) and precipitating with pentane (30 mL) afforded **4a** as a red solid which was still contaminated with significant amounts of **2c**. ¹H NMR (acetone-*d*₆): δ = 7.12 (s, 2H, C₆H₂), 4.93 (d, 2H, ²J_{HH} = 13.2 Hz, CH₂N, lowfield part of ABq), 3.62 (d, 2H, ²J_{HH} = 12.9 Hz, CH₂N, highfield part of ABq), 3.46 (q, 2H, ³J_{HH} = 7.2 Hz, CCH₂CH₃), 3.11 (s, 6H, ³J_{PH} not resolved, NCH₃Me), 2.77 (s, 6H, ³J_{PH} not resolved, NMeCH₃), 0.63 (t, 3H, ³J_{HH} = 7.4 Hz, CCH₂CH₃).

[PtCl(C₆H₂{CH₂C₆H₅}-1-{CH₂NMe₂})₂-2,6-OH-4)](BF₄) (5a**). To a stirred solution of **2b** (0.35 g, 0.69 mmol) in acetone (10 mL) was poured BnCl (4 mL, 35 mmol) which caused a slow colorization to orange. After 12 h, the formed precipitate was removed by filtration and the filtrate evaporated in vacuo. The crude product was precipitated from CHCl₃/Et₂O to yield **5a** as a yellow solid (0.28 g, 67%). ¹H NMR (acetone-*d*₆): δ = 7.1–6.8 (m, 5H, C₆H₅), 6.96 (s, 2H, C₆H₂), 5.10 (d, 2H, ²J_{HH} = 13.2 Hz, ³J_{PH} = 48.8 Hz, CH₂N, lowfield part of ABq), 4.77 (s, 2H, ³J_{PH} not resolved, CCH₂Ar), 3.71 (d, 2H, ²J_{HH} = 13.4 Hz, ³J_{PH} = 39.7 Hz, CH₂N, highfield part of ABq), 3.06 (s, 6H, ³J_{PH} = 27.9 Hz, NCH₃Me), 2.78 (s, 6H, ³J_{PH} = 29.6 Hz, NMeCH₃); ¹³C {¹H} NMR (acetone-*d*₆): δ = 173.1 (C_{para}), 161.5 (C_{ortho}), 129.2, 127.8, 127.5 (all C₆H₅), 118.7 (C_{meta}), C_{ipso} not observed, 68.9 (CH₂N), 53.7 (NCH₃-Me), 51.9 (NMeCH₃), 39.6 (CCH₂Ar); Anal. Calcd for C₁₉H₂₆BClF₄N₂OPt (615.78): C, 37.06; H, 4.26; N, 4.55. Found: C, 38.14; H, 4.55; N, 4.50.**

[PtBr(C₆H₂{CH₂C₆H₅}-1-{CH₂NMe₂})₂-2,6-OH-4)](BF₄) (5b**). Addition of BnBr (3 mL, 25 mmol) to **2b** (0.45 g, 0.89 mmol) in acetone (10 mL) afforded a purple solution within 15 min. Analysis of this intermediate **9**: ¹H NMR (acetone-*d*₆): δ = 7.15–6.90 (m, 5H, C₆H₅), 6.80 (s, 2H, C₆H₂), 5.04 (d, 2H, ²J_{HH} = 13.2 Hz, CH₂N, lowfield part of ABq), 4.61 (s, 2H, ²J_{PH} = 24 Hz, CCH₂Ar), 3.58 (d, 2H, ²J_{HH} = 13.5 Hz, CH₂N, highfield part of ABq), 3.11 (s, 6H, ³J_{PH} = 32.6 Hz, NCH₃Me), 2.83 (s, 6H, ³J_{PH} = 28.5 Hz, NMeCH₃). Within 1 h, the color of the reaction solution changed to orange, and after additional 1 h of stirring, the volatiles were removed by evaporation under reduced pressure. The crude product was isolated by repetitive precipitation of a CH₂Cl₂ solution with pentane and was finally recrystallized from CHCl₃/Et₂O to yield **5b** as an orange solid (0.48 g, 81%). ¹H NMR (acetone-*d*₆): δ = 7.1–6.8 (m, 5H, C₆H₅), 6.44 (s, 2H, C₆H₂), 5.11 (d, 2H, ²J_{HH} = 13.2 Hz, CH₂N, lowfield part of ABq), 4.85 (s, 2H, ³J_{PH} = 30 Hz, CCH₂Ar), 3.72 (d, 2H, ²J_{HH} = 13.7 Hz, CH₂N, highfield part of ABq), 3.10 (s, 6H, ³J_{PH} not resolved, NCH₃Me), 2.78 (s, 6H, ³J_{PH} = 37.2 Hz, NMeCH₃); ¹³C {¹H} NMR (acetone-*d*₆): δ = 172.5 (C_{para}), 157.5 (C_{ortho}), 129.3, 129.1, 127.6, 127.5 (all C₆H₅), 118.4 (C_{meta}), 79.8 (C_{ipso}), 68.2 (CH₂N), 55.0 (NCH₃Me), 52.9 (NMeCH₃), 39.3 (CCH₂Ar); Anal. Calcd for C₁₉H₂₆BBtF₄N₂OPt (660.23): C, 34.57; H, 3.97; N, 4.24. Found: C, 34.72; H, 4.03; N, 4.29.**

[PtBr(C₆H₂{CH₂C₆H₅}-1-{CH₂NMe₂})₂-2,6-OMe-4)](SO₃CF₃) (5c**). Addition of BnBr (1 mL, 8 mmol) to **2b** (0.19 g, 0.36 mmol) in acetone (4 mL) afforded a purple solution within 10 min, which subsequently turned orange (1.5 h). The volatiles were removed in vacuo, and the product was purified by repetitive crystallization from acetone/pentane solution, which yielded **5c** as orange crystals (0.16 g, 65%). ¹H NMR (acetone-*d*₆): δ = 7.29 (s, 2H, C₆H₂), 7.15–7.12 (m, 3H, C₆H₅), 6.89–6.85 (m, 2H, C₆H₅), 5.17 (d, 2H, ²J_{HH} = 13.3 Hz, CH₂N, lowfield part of ABq), 4.97 (s, 2H, ³J_{PH} not resolved, CCH₂Ar), 4.21 (s, 3H, OMe), 3.84 (d, 2H, ²J_{HH} = 13.4 Hz, CH₂N, highfield part of ABq), 3.12 (s, 6H, ³J_{PH} = 29.4 Hz, NCH₃Me), 2.79 (s, 6H, ³J_{PH} = 24.2 Hz, NMeCH₃); ¹³C {¹H} NMR (acetone-*d*₆): δ = 171.1 (C_{para}), 154.2 (C_{ortho}), 140.5, 129.5, 127.7, 127.6 (all C₆H₅), 117.1 (C_{meta}), 83.4 (C_{ipso}), 69.3 (CH₂N), 59.0 (OMe), 55.2 (NCH₃Me), 53.0 (NMeCH₃), 39.0 (CCH₂Ar).**

[Pt(C₆H₂{Me₃Si}-1-{CH₂NMe₂})₂-2,6-OSiMe₂Bu-4)](CF₃SO₃) (6a**). To a solution of [Pt(C₆H₂{CH₂NMe₂})₂-2,6-OSiMe₂Bu-4)] (0.11 g, 0.2 mmol) in dry CH₂Cl₂ (3 mL) was added excess Me₃SiOTf (0.8 mL, 4 mmol). Immediately, the solution turned dark red. When this solution was layered with dry pentane, a white crystalline solid was obtained together with some decomposition products. The crystalline material**

showed spectroscopic properties identical to those of the platinum(II) starting material. However, carrying out the same reaction in CD₂Cl₂ allowed for spectroscopic analysis of **6a**. ¹H NMR (CD₂Cl₂): δ = 7.09 (s, 2H, C₆H₂), 4.25 (d, 2H, ²J_{HH} = 12.9 Hz, CH₂N, lowfield part of ABq), 3.40 (d, 2H, ²J_{HH} = 12.8 Hz, CH₂N, highfield part of ABq), 3.04 (s, 6H, ³J_{PH} not resolved, NCH₃Me), 2.72 (s, 6H, ³J_{PH} not resolved, NMeCH₃), 1.00 (s, 9H, CCH₃), 0.69 (s, 9H, Me₃Si), signal of Me₂Si not resolved due to overlap with the resonances of residual Me₃SiOTf; ²⁹Si NMR (CD₂Cl₂): δ = 78.9 (Me₃Si-arenium), 9.64 (Me₂BuSi-O).

[PtCl(C₆H₂{Me₃Si}-1-{CH₂NMe₂})₂-2,6-OSiMe₂Bu-4)](CF₃SO₃) (6b**). To a solution of **2b** (0.06 g, 0.1 mmol) in dry CD₂Cl₂ (0.7 mL) was added excess Me₃SiOTf (0.1 mL, 0.5 mmol). Immediately, the solution turned dark orange. ¹H NMR (CD₂Cl₂): δ = 7.05 (br s, 2H, C₆H₂), 3.99 (br s, 4H, CH₂N), 3.00 (br s, 6H, ³J_{PH} not resolved, NCH₃-Me), 2.77 (br s, 6H, ³J_{PH} not resolved, NMeCH₃), 1.01 (s, 9H, CCH₃), 0.69 (s, 9H, Me₃Si), signal of Me₂Si not resolved due to overlap with the resonances of residual Me₃SiOTf.**

[Pt(C₆H₂{Me}-1-{CH₂NMe₂})₂-2,6-O-4)] (7**). **Procedure A.** A solution of **3b** (0.70 g, 1 mmol) in THF (5 mL) was treated with excess NEt₃ (1.4 mL, 10 mmol), which immediately caused a color change of the solution from dark red to yellow. Toluene (20 mL) was added and the suspension filtered. Evaporation of the filtrate gave **7** as a yellow solid (0.53 g, 98%). **Procedure B.** Aqueous NaOH (4 M, 0.5 mL, 2 mmol) was added to a solution of **3c** (0.71 g, 1 mmol) in THF (5 mL). The reaction mixture became immediately yellow and was stirred for 30 min. After addition of NaOH (1 M, 15 mL) and toluene (20 mL), the organic phase was separated and the aqueous layer extracted with toluene (2 × 15 mL). The combined organic layers were dried over Na₂SO₄ and filtered, and the solvent was removed under reduced pressure. Slow precipitation from CH₂Cl₂/pentane afforded **7** as a microcrystalline yellow solid (0.77 g, 71%). ¹H NMR (CDCl₃): δ = 6.07 (s, 2H, ⁴J_{PH} = 16 Hz, C₆H₂), 4.22 (s, 2H, ²J_{HH} = 13.5 Hz, lowfield part of ABq), 3.05 (s, 6H, ³J_{PH} = 38.8 Hz, NMeCH₃), 2.94 (s, 6H, ³J_{PH} = 40.5 Hz, NCH₃Me), 2.81 (s, 2H, ²J_{HH} = 13.2 Hz, ³J_{PH} = 54.2 Hz, CH₂N, highfield part of ABq), 1.54 (s, 3H, ³J_{PH} = 51.2 Hz, CCH₃); ¹³C {¹H} NMR (CDCl₃): δ = 187.5 (C_{para}), 163.0 (C_{ortho}), 119.7 (²J_{PH} = 24.3 Hz, C_{meta}), 70.4 (CH₂N), 56.2 (²J_{PH} = 12 Hz, NMeCH₃), 55.0 (²J_{PH} = 21 Hz, NMeCH₃), 49.1 (C_{ipso}), 23.5 (²J_{PH} = 97 Hz, CCH₃); ¹⁷O NMR (THF): δ = 450; Anal. Calcd for C₁₃H₂₁IN₂O (543.31): C, 28.42; H, 4.95; N, 5.10. Found: C, 28.55; H, 5.05; N, 5.13.**

(C₆H₂{Bn}-4-{CH₂NMe₂})₂-3,5-OH-1 (8b**). A solution of **5b** (15.4 mg, 23 μmol) in CH₂Cl₂ (5 mL) was vigorously stirred with an aqueous solution of KCN (0.5 M, 6 mL, 3 mmol) for 4 h. Aqueous NaOH (2 M, 5 mL) was added, and the product was extracted with CH₂Cl₂ (3 × 5 mL). The combined organic fractions were washed with brine (10 mL), dried over MgSO₄, and evaporated to dryness to afford a yellowish oil (6.5 mg, 94%). ¹H NMR (CDCl₃): δ = 7.22–6.95 (m, 5H, C₆H₅), 6.84 (s, 2H, C₆H₂), 4.24 (s, 2H, CCH₂Ar), 3.25 (s, 4H, CH₂N), 2.18 (s, 12H, NCH₃); OH not observed; ¹³C {¹H} NMR (CDCl₃): δ = 154.3, 141.1, 139.0, 129.8, 128.4, 127.9, 125.7, 116.3 (all C_{aryl}), 61.6 (CH₂N), 45.3 (NMe₂), 32.4 (CH₂).**

(C₆H₂{Me}-4-{CH₂NMe₂})₂-3,5-OH-1 (8a**). The procedure was similar to that of **8b**, starting from a solution of **3c** (0.07 g, 0.1 mmol) in CH₂Cl₂ (5 mL) and aqueous KCN (0.5 M, 6 mL, 3 mmol), giving the title product as a yellowish oil (13 mg, 60%).**

¹H NMR (CDCl₃): δ = 6.15 (s, 2H, C₆H₂), 3.50 (s, 4H, CH₂N), 2.22 (s, 12H, NCH₃), 1.72 (s, 3H, ArCH₃); OH not observed.

Reaction of [Pt(C₆H₂{CH₂NMe₂})₂-2,6-OH-4](OH₂)](CF₃SO₃) (2a**) with HCl.** A solution of **2a** (40 mg, 0.07 mmol) in acetone-*d*₆ (2 mL) was treated with freshly prepared gaseous HCl. The color of the mixture turned orange, and a white precipitate formed, which was removed by filtration. Analysis of the orange solution: ¹H NMR (acetone-*d*₆): δ = 5.92 (s, 2H, C₆H₂), 4.41 (s, 2H, ³J_{PH} = 30.3 Hz, CH₂N), 4.00 (s, 2H, ³J_{PH} = 45.9 Hz, CH₂N), 3.02 (s, 6H, ³J_{PH} = 29.5 Hz, NMe₂), 3.00 (s, 6H, ³J_{PH} = 38.7 Hz, NMe₂). Evaporation of the orange filtrate afforded a dark oily residue. The ¹H NMR data of this product are identical with those of the starting material **2a**.

Structure Determination and Refinement of **3c and **5c**.** X-ray data were collected on an Enraf-Nonius CAD4-T diffractometer with rotating anode (Mo Kα radiation, λ = 0.71073 Å). Crystal data and details on data collection and refinement are given in Table 3. The

Table 3. Crystallographic Data for **3c** and **5c**

	3c	5c
color, shape	red cube	orange cube
empirical formula	C ₁₅ H ₂₄ F ₃ IN ₂ O ₄ PtS	C ₂₁ H ₂₈ BrF ₃ N ₂ O ₄ PtS ^a
formula weight	707.41	736.50 ^a
radiation/Å	Mo Kα (monochr.) 0.71073	Mo Kα (monochr.) 0.71073
T/K	150	150
crystal system	monoclinic	monoclinic
space group	<i>P</i> 2 ₁ / <i>c</i> (No. 14)	<i>P</i> 2 ₁ / <i>c</i> (No. 14)
unit cell dimensions		
<i>a</i> /Å	10.9657(12)	12.0016(16)
<i>b</i> /Å	15.9029(14)	17.7331(10)
<i>c</i> /Å	11.9313(11)	15.008(2)
β /deg	93.304(8)	115.263(10)
<i>V</i> /Å ³	2077.2(3)	2888.6(6)
<i>Z</i>	4	4
<i>D</i> _{calc} /g cm ⁻³	2.262	1.694 ^a
μ /mm ⁻¹ (Mo Kα)	8.391	6.358 ^a
crystal size/mm	0.4 × 0.2 × 0.1	0.48 × 0.38 × 0.38
(<i>sin</i> θ/λ) _{max} /Å ⁻¹	0.65	0.65
total, unique reflcns	3984, 3644	7108, 6579
<i>R</i> _{int}	0.059	0.034
transmission range	0.171–0.643	0.362–0.776
parameters, restraints	250, 0	303, 0
<i>R</i> ₁ ^b , <i>wR</i> ₂ ^c , <i>S</i>	0.0400, 0.0959, 1.046	0.0395, 0.0962, 1.01
<i>w</i> ^{-1 d}	$\sigma^2(F_o^2) + (0.0494P)^2$	$\sigma^2(F_o^2) + (0.0525P)^2$
resid. density/e Å ⁻³	−0.77 < 0.83	−0.93 < 1.12

^a Excluding disordered solvent molecules in the voids. ^b $R_1 = \sum ||F_o| - |F_c|| / \sum |F_o|$, for all $I > 4\sigma(I)$. ^c $wR_2 = [\sum [w(F_o^2 - F_c^2)^2] / \sum [w(F_o^2)^2]]^{1/2}$. ^d $P = (\max(F_o^2, 0) + 2F_c^2) / 3$.

structures were solved with Patterson methods (DIRDIF-97⁴³) and refined against F^2 of all reflections (SHELXL-97⁴⁴). Non-hydrogen atoms were refined freely with anisotropic displacement parameters;

hydrogen atoms were refined at calculated positions riding on their carrier atoms. Weights were optimized in the final refinement cycles. The unit cell of **5c** contains two solvent accessible voids of 311 Å³ each. Disordered solvent molecules in the voids were taken into account by back Fourier transformation (PLATON/SQUEEZE).⁴⁵ Neutral atomic scattering factors and anomalous dispersion corrections were taken from the *International Tables of Crystallography*. All other calculations, graphical illustrations, and checking for higher symmetry were performed with the PLATON package.⁴⁵

Acknowledgment. We gratefully acknowledge Dr. P. J. Davies (Utrecht University) for preparing complexes **2b** and **2d**, and Dr. U. Frey (Université de Lausanne) for performing the ¹⁷O NMR measurements. This work was supported in part (A.L.S.) by the Dutch Council for Scientific Research (CW-NWO).

Supporting Information Available: Listing of the temperature-dependent equilibrium constants of **5b** and **9** (PDF) and X-ray structural information on **3c** and **5c** (CIF). This material is available free of charge via the Internet at <http://pubs.acs.org>.

JA003685B

(43) Beurskens, P. T.; Admiraal, G.; Beurskens, G.; Bosman, W. P.; Garcia-Granda, S.; Gould, R. O.; Smits, J. M. M.; Smykalla, C. *The DIRDIF program system*, Technical report of the Crystallography Laboratory; University of Nijmegen: The Netherlands, 1997.

(44) Sheldrick, G. M. *SHELXL-97*, Program for crystal structure refinement; University of Göttingen: Germany, 1997.

(45) Spek, A. L. *PLATON*, A Multipurpose Crystallographic Tool; Utrecht University: The Netherlands, 2000.